To the Graduate Council:

I am submitting herewith a thesis written by Samuel Held entitled "J/ψ Production and Absorption in High Energy Nuclear Collisions." I have examined the final copy of this thesis for form and content and recommend that it be accepted in partial fulfillment of the requirements for the degree of Master of Science, with a major in Physics.

Soren P. Sorensen, Major Professor

We have read this thesis
and recommend its acceptance:

Accepted for the Council:

Associate Vice Chancellor
and Dean of the Graduate School

J/ψ Production and Absorption in High Energy Nuclear Collisions

A Thesis

Presented for the

Master of Science Degree

The University of Tennessee, Knoxville

Samuel Held

August 1999

Acknowledgments

The first and biggest thank you goes deservingly to my wife, Erica. Without her, I would never have ended up at Tennessee or made it through graduate school. Also, lots of thanks to my son, Sammy, who gave me a new sense of direction in my life and for making me truly happy.

I also wish to thank Dr. Soren Sorensen, who hired a prospective graduate student mostly because he had heard of PHENIX before coming to UT. Thank you for teaching me the intricacies of nuclear physics and being supportive throughout this entire process.

Thanks to Dr. Ken Read for teaching me about the physics involved in the PHENIX Muon Arm. To Dr. Kyle Pope, Saskia Mioduszewski, Jason Newby, Andrew Glenn, Korey Sorge, Darren Ellis, and Steve McDaniel, thanks for many interesting discussions on so many different topics.

I also wish to thank Ted Corcovilos for porting SPACY to LINUX, helping to set up and carry out the large amount of runs to carry this thesis, and also for many interesting conversations about physics. Good luck at Cal Tech.

Thanks to members of the HERG Group at Oak Ridge National Lab: Terry, Vince, Yuri, Yuri, Frank, Paul, and Glenn for answering my many questions about the details of RHIC physics and then giving me even more questions.

Last but not least, I wish to thank the rest of my friends and family for all their support through my entire life, not just school.

Abstract

We used a computer code, called SPACY, to simulate the production and absorption of the J/ψ meson in nucleus-nucleus collisions. This simulation was carried out in a purely hadronic scenerio assuming that the nucleus-nucleus collision is an aggregate of hadron-hadron collisions. This was used to analyze a possible hadronic explanation for the results from CERN experiment NA50. These results showed an "anomalous" suppression of the J/ψ meson in Pb+Pb collisons at 158 A GeV/c along with a threshold in the transverse energy distribution. Predictions from SPACY cannot explain with the hadronic scenario either the "anomalous" suppression or the threshold in the E_T distribution. We also find that one cannot determine the octet versus singlet contributions to the absorption without further data.

Contents

List of Tables

List of Figures

Chapter 1

Introduction

This thesis investigates the phenomenon of J/ψ suppression through the use of a purely hadronic scenario. This study is carried out with the use of a Monte Carlo simulation cascade code called SPACY, which simulates the hadronic environment of a collision region. This code creates the J/ψ meson and follows its journey in full space-time through the collision region. We will compare the predictions of SPACY to the experimental results of experiment NA50 at CERN which used Pb+Pb collisions at 158 A GeV/c to study J/ψ suppression.

1.1 High-Energy Nuclear Physics

The ultimate goal of high-energy nuclear physics is confirmation of a prediction of Quantum Chromodynamics (QCD): that in a volume of hot and dense matter, the quarks and gluons will become deconfined. This "melting" of nucleons into

their constituent quarks and gluons is a phase transition from hadronic (confined) matter to quark (deconfined) matter, also called the formation of a quark-gluon plasma (QGP). This new state of matter is called a plasma because the deconfined quarks, antiquarks, and gluons resemble a charged gas with Coulomb-like interactions. It is predicted that this state of matter existed in the early universe up to 10^{-6}s after the Big Bang. Theorists have been making predictions of experimental signatures for detection and study of the QGP since the early 1980's. These signals include strangeness enhancement, low mass dilepton enhancement, heavy vector meson suppression, and increased direct photon production [8].

The most promising terrestial environment to produce the large energy densities necessary to form a QGP ($\sim$2-3 GeV/fm^3) is a nucleus-nucleus collision. This large energy density is the result of the accumulation of energy from each individual nucleon involved in the collision. Lattice QCD predicts that the QGP will form at temperatures between 150-200 GeV and/or nuclear densities about five to ten times normal nuclear density [8]. This QGP lives for only about 3-10 fm/c (which is equivalent to $(1-3)$ x 10^{-23} s) because the volume expands causing the energy density to drop to the point where the quarks and gluons are again confined to hadrons. This process is called hadronization. Thus, experiments will primarily see the effects of secondary collisions. We would like to study the initial state of the collision that tells us about the QGP directly. This means these signals have to survive the journey through the collision region.

1.2 Signatures of Quark-Gluon Plasma Formation

It is widely accepted in the high-energy nuclear physics community that observation of one of the predicted signals of QGP production does not conclusively prove the existence of the parton-hadron phase transition. So, we must look for a variety of signals. This section gives a short introduction to five of the predicted signals, including the focus of this thesis, vector meson suppression. For further reading on the material, please refer to C.-Y. Wong's book [8] and the references therein.

1.2.1 Strangeness Enhancement

The number of particles containing strange quarks is predicted to be enhanced [9], when a QGP is formed. In hadronic matter, the ratio of $s\bar{s}$ pair production to nonstrange $q\bar{q}$ pair production is about 0.1 ($q\bar{q}$ represents $u\bar{u}$ and $d\bar{d}$). One way to gauge an increase in the $s\bar{s}/u\bar{u}d\bar{d}$ ratio is to measure the K^+/π^+ ratio, especially because the produced hadrons in the collisions consist mostly of pions and kaons.

As the temperature of a hadron gas in thermal and chemical equilibrium increases, the pion and kaon densities rise as well. However, the kaon density increases at a rate faster than the pion density. Thus, some of the increase of the K^+/π^+ can be explained in a hadronic scenario. Thermal equilibrium is achieved when the momentum distributions of the particles reach a dynamic equilibrium.

Chemical equilibrium is reached when the densities of different particles reach a steady state (also a dynamic equilibrium).

Early work predicts [10] that at a temperature T=200 MeV, the reaction rate in the collisions is not fast enough for a hadron gas to reach chemical equilibrium, because the strange quark threshold energy is large compared to the temperature. Since this work was done in 1986, more work has been done on this topic and suggestions have been made to explain how chemical equilibrium can be reached. Brown *et al* [11] proposes that the strange quark mass lowers as the temperature approaches the phase transition temperature. This would lead to higher amounts of $s\bar{s}$ pair production. This would lead to higher amounts of hadrons with strange content in a hadronic scenario. Another proposal by R. Matiello *et al* [12] predicts that higher (mass) resonance interactions with nucleons contribute to the various particle species densities thus reducing the time to reach a steady state. There is currently more work under way to help reconcile the theoretical predictions and experimental results.

In a QGP, the strange quark mass and the temperature of the collision region are roughly the same magnitude. This means that the strange quarks and anti-quarks are produced at a higher rate and that leads to a larger number of mesons with s and $\bar{s}$ content. This large temperature also leads to an increased production of $\bar{u}$ and $\bar{d}$. With equal numbers of quarks and antiquarks, the probabilities for production of antihyperons and nonstrange antibaryons ($\bar{u}, \bar{d}, \bar{s}$ combinations) and

hyperons and nonstrange baryons (u, d, s combinations) are equilibrated. Hyperons (or antihyperons) are baryons with one or more strange quark (or antiquark) as members of their constituent quarks (or antiquarks).

This scenario is contrary to what happens in hadronic matter. There the densities of u and d are greater than $\bar{u}$ and $\bar{d}$ densities, so meson production is more likely than baryon or antibaryon production. Since mesons consist of $q\bar{q}$ pairs, the strange antiquarks will combine with the u and d quarks to form $K^+(u\bar{s})$ or $K^0(d\bar{s})$ mesons. This production is much more likely than $\bar{K^0}(\bar{u}s)$ and $K^-(\bar{d}s)$ production, because of the low number of $\bar{u}$ and $\bar{d}$ antiquarks. For the s quarks, it is more likely they form with u and d quarks to make $\Lambda(uds), \Sigma^+(uus), \Sigma^0(uds)$, and $\Sigma^-(dds)$ baryons. Thus there is a hadronic enhancement to the K^+/π^+ ratio, so experimentalists look for an increase beyond the hadronic contributions.

1.2.2 Low Mass Dilepton Enhancement

In a QGP, a quark q and an antiquark $\bar{q}$ can interact to form a virtual photon γ^*, which subsequently decays into a lepton l^- and an antilepton l^+ (a dilepton pair). After these dileptons form, they must pass through the collision region to the particle detectors. Since they interact only through the electromagnetic force, their free mean path is quite large. That means that the leptons are not likely to suffer further collisions after they are produced. On the other hand, the production rate and momentum distribution of the produced dilepton pair depends on

the momentum distribution of the quarks and antiquarks in the plasma, which is governed by the thermodynamic condition of the plasma. Therefore, the dilepton pairs carry information on the thermodynamical state of the medium at the moment of their production. One can conceivably use this to view the initial state of the collision [8].

There are hadronic processes which could serve as background by increasing the dilepton yield. One such process is the Drell-Yan process, which produces a dilepton pair. A valence quark of a nucleon of one nucleus can interact with a sea antiquark of a nucleon of another nucleus. They annihilate to form a virtual photon, which subsequently decays into a dilepton pair. The number of l^+l^- pairs from the Drell-Yan process for central collisions of two equal size nuclei scales as $A^{4/3}$. These facts are important for the Pb+Pb collisions that NA50 observes, because they use Drell-Yan dileptons as a reference process. It plays an important role as a background process on the upper edge of the low dimuon invariant mass region (about 1.5 GeV).

We also have to consider dilepton pairs from the annihilation of charged hadrons and their antiparticles. An example process is

$$\pi^+ + \pi^- \rightarrow l^+ + l^-. \tag{1.1}$$

We also have to consider decays of hadron resonances such as the ρ, ω, and ϕ. One

of the difficulties with these background processes is that it occurs whether or not a QGP forms. Estimates of the l^+l^- pairs that come from hadronic sources can be based only on the pions because they dominate the produced hadronic matter. This process is

$$\pi^+ + \pi^- \rightarrow \gamma^* \text{or} \rho \rightarrow l^+ l^- \tag{1.2}$$

where the path with γ^* can be calculated with scalar electrodynamics, and the path with the ρ meson can be calculated with the vector dominance model [8]. These decays of the hadron resonances can show up as broad peaks (closer to being bumps) in the low mass region of the dilepton's invariant mass spectrum.

We must also consider the dilepton pair contribution from charm production, more specifically open charm production. The $c\bar{c}$ pair is produced and the c quark combines with a $\bar{u}, \bar{d}$, or $\bar{s}$ quark to form a D^+ meson while the $\bar{c}$ quark combines with a u, d, or s quark to form a D^- meson. The D^+ meson decays into $l^+ \bar{K}^0 \nu_l$ while the D^- meson decays into $l^- K^0 \bar{\nu}_l$, giving us a background dilepton pair.

1.2.3 Direct Photon Production

If a quark-gluon plasma is produced, more than likely it will be formed at a higher temperature than the hadronic gas that would exist if the QGP was not formed. Since both of these systems radiate photons at a rate that goes like T^4, the plasma will "shine" brighter when it emits more photons than the gas. Hence

in a quark-gluon plasma, there is a predicted enhancement of photon production.

There are two processes for direct photon production in a quark-gluon plasma, annihilation

$$q + \bar{q} \rightarrow \gamma + g \tag{1.3}$$

and the Compton process

$$g + q(\bar{q}) \rightarrow \gamma + q(\bar{q}). \tag{1.4}$$

The annihilation process involves the production of the gluon instead of 2γ, because the latter process is suppressed by a factor (α_e/α_s), where $\alpha_s \gg \alpha_e$. (The α_s variable is the strong force coupling constant and α_e is the electromagnetic force coupling constant.) The Compton process is named such because it resembles Compton scattering, which is the scattering of a photon off a charged particle. After a photon is produced, it must make it out of the collision region and does so because it interacts with other particles exclusively through the electromagnetic force. The photon is similar to a dilepton in this manner and thus the same result applies: since its mean free path through the collision region is large, its exit from the region is very possible. Also, the momentum distribution of the photons will reflect the momentum distributions of the quarks and antiquarks, which tell us about the thermodynamical state of the QGP [8].

When the energy of the produced photon is much greater than rest mass of the quark or antiquark ($E_\gamma \gg m_o$), then the annihilation process and Compton

process share similar results. First, the photon is produced in a very narrow cone along the direction of the original quark or antiquark. Second, the momentum of the photon is almost exactly that of the original quark or antiquark. These two results lead to the interpretation that the production of the photon can be viewed as the original quark or antiquark turning itself into a photon. This also means that the Compton process probes only the quark and antiquark distribution.

There are hadronic processes that mimic direct photon production in a QGP, which include hadron interactions. One such set of processes is pion interactions, which include pion annihilation

$$\pi^+ + \pi^- \rightarrow \gamma + \rho^0, \tag{1.5}$$

charged pion interaction with a neutral pion

$$\pi^\pm + \pi^0 \rightarrow \gamma + \rho^\pm, \tag{1.6}$$

or pion interactions with ρ mesons

$$\pi^\pm + \rho^0 \rightarrow \gamma + \pi^\pm, \tag{1.7}$$

$$\pi^\pm + \rho^\mp \rightarrow \gamma + \pi^0, \tag{1.8}$$

and

$$\pi^0 + \rho^{\pm} \rightarrow \gamma + \pi^{\pm}. \tag{1.9}$$

Since the hadronic interactions occur at a lower temperature than those found in a quark-gluon plasma, the distribution of the photons will reflect this. Kapusta *et al* [13] predicted that if a QGP and a hadron gas have the same temperature (200 MeV in the paper) then the shapes of the spectra for the photons are nearly the same at high photon energies. They concluded that the temperature of a hadron gas is slightly higher than that of a QGP, which means that a hadron gas "shines as brightly as (or even slightly brighter than) a quark-gluon plasma" [13]. Realistically, this situation will not occur very often. So the temperature of the system should be able to distinguish between a hot QGP and a cooler hadronic gas.

Two of the experiments that have made photon measurements at CERN are WA80 and NA45. WA80 observed photons directly with their lead-glass calorimeter, where the photons mostly came from the decays of π^0 or η mesons. Knowing their production yields, WA80 looked at photon production above this magnitude and away from the meson peaks in the energy spectrum. The WA80 experiment claims to have seen enhanced photon production in central collisions for $p_T < 2$ GeV, with an experimental error of $5.8 - 7.9\%$ [14]. On the other hand, NA45 used a material to convert the photons into electron and positron pairs and then mea-

sured those particles in a ring imaging Čerenkov spectrometer. They did not see the photon excess that WA80 did but their systematic error was 11% [15]. These conflicting results need to be independently checked with another experiment.

1.2.4 Vector Meson Suppression

Even though the theory presented in this subsection can be expanded to other high mass vector mesons such as the $\Upsilon(1S)$ and its higher states. I will consider only charmonium, specifically the 1S state (J/ψ) and the 2S state (ψ'). At current colliders for high-energy nuclear collisions, the J/ψ is produced copiously but the Υ suffers from poor statistics.

In a quark-gluon plasma, the string tension between two quarks becomes zero, which means that a charm quark and charm antiquark will have a Coulomb-type color interaction between them. In the deconfined environment of a QGP, the color charge of the charm quark will be screened from the charm antiquark by the quarks, antiquarks, and gluons of the plasma. This screening again modifies the interaction of the charm quark and charm antiquark from the Coulomb-type

$$V(r) = \frac{q}{4\pi r} \tag{1.10}$$

to a short-range Yukawa-type interaction with a range, λ_D

$$V(r) = \frac{q}{4\pi}\frac{e^{-r/\lambda_D}}{r}. \tag{1.11}$$

This screening is called Debye screening and λ_D is called the Debye screening length. If the separation of the charm quark and charm antiquark, $r_{c\bar{c}}$, is less than the Debye screening length, $r_{c\bar{c}} < \lambda_D$, then a bound state of the $c\bar{c}$ can be formed. However, if $r_{c\bar{c}} > \lambda_D$, then the c and $\bar{c}$ quarks will not together form a bound state but will separately bind with light quarks and antiquarks of the plasma to form D mesons, open charm. These D mesons are discussed above.

Shortly after the initial proposal of J/ψ suppression as a signal of deconfinement [16] in 1986, the NA38 Collaboration at CERN observed a suppression of J/ψ production relative to the dimuon continuum [17] in central collisions of ^{16}O projectiles on an ^{238}U target at 200 A GeV/c[1]. NA38 actually measured the $N_{J/\psi}/N_{cont}$ and saw a decrease as predicted by Matsui and Satz [16]. ($N_{J/\psi}$ is the number of dimuons with an invariant mass near the J/ψ mass and N_{cont} is the number of dimuons with an invariant mass away from the J/ψ mass.) However to conclude with certainty that this indicates a QGP means that hadronic scenarios

[1]The symbol A GeV/c represents that amount momentum each nucleon in the projectile possesses.

must be ruled out completely. So interactions like

$$J/\psi + h \rightarrow D + \bar{D} + X, \tag{1.12}$$

must be ruled out as the source of the suppression, as well as all other non-QGP explanations. A hadronic scenario of suppression is the major topic of this thesis. More details about J/ψ suppression will be discussed in the next chapter.

1.3 Global and Other Variables in Nuclear Collisions

The global variables are those physical quantities which experimentalists use to characterize entire events (collisions). They include transverse energy, charged particle multiplicity, and the forward energy. Physicists use an energy-related vector in their data analysis. They look at how much energy is carried transversely or longitudinal to the beam axis by adding up the energy of particles that travel along that respective direction. The definition of transverse energy is

$$E_T = \sum_i E_i \cdot \sin\theta_i, \tag{1.13}$$

where E_i is the total energy of the i^{th} particle and θ_i is the polar angle that the i^{th} particle has to the beampipe (z- axis). In experiments, this energy is measured by calorimeters (hadronic or electromagnetic), which measure the energy differently

for different particles. For most particles, such as the $p, n, \pi^{\pm}, K^{\pm}$, and $K^0_{L,S}$, the energy that is deposited in the hadronic calorimeter is the kinetic energy of the particle, $E_i = T_i$. For the π^0, the entire energy of the particle is deposited into an electromagnetic calorimeter, because it decays very quickly (10^{-17}s) into two photons which deposit all their energy in the electromagnetic showers in the calorimeter. For the $\bar{p}$ and $\bar{n}$, the energy is the kinetic energy of the antibaryon plus twice its rest mass (m_o) due to the annihilation with a baryon in the calorimeter, $E_i = T_i + 2m_{o_i}$. The charged particle multiplicity is the total number of charged particles produced in each event (collision). The charged particles are the ones that can be detected by multiplicity detectors that usually consist of ionization and scintillation detectors. The forward energy (sometimes abbreviated E_F) is also called the zero-degree energy, E_{ZDC}, in reference to the particle's direction along the beam direction (the longitudinal direction). It is the sum of the kinetic energy of the particles that go forward in a very narrow cone, usually polar angle $\theta < 0.3^o$,

$$E_F = \sum_i T_i. \tag{1.14}$$

Both E_T and E_F are commonly used to characterize the centrality of a collision, which in turn is used to extract the impact parameter range of the colliding particles (nuclei or nucleons).

We use other variables that are specific to particles and even particle species

(i.e., pions or kaons) in collisions, which include transverse momentum, rapidity, and pseudorapidity. Transverse momentum, p_T, is a combination of the x and y components of the total momentum,

$$p_T = \sqrt{p_x^2 + p_y^2}. \tag{1.15}$$

This gives only two components for momentum, one transverse to the beam and one longitudinal. Rapidity is a measure of a particle's velocity that lends itself nicely to relativistic frame transformations. The equation for rapidity is given by

$$y = \frac{1}{2}\left(\ln \frac{E + p_z}{E - p_z}\right). \tag{1.16}$$

Pseudorapidity is a variable that characterizes the angular distributions of the particles that are created by the collision. For a particle with $E \gg m_o$ (relativistic), the pseudorapidity is approximately equal to the rapidity, but is easier to measure with particle detectors. The equation for pseudorapidity is

$$\eta = -\ln\left(\tan \frac{\theta}{2}\right). \tag{1.17}$$

1.4 The J/ψ as a Probe

1.4.1 Properties of the J/ψ

The J/ψ meson is the bound state of a charm quark c and a charm antiquark $\bar{c}$. The radius of the bound state is the size of the J/ψ and is given by $r_{J/\psi} = \frac{1}{2m_c}$, where m_c= 1.5 GeV/c^2 is the mass of the charm quark. Since $r_{J/\psi} \simeq 0.20$ fm is so small, the bound state is tightly bound and hard to break apart. If the J/ψ were broken apart, the charm quark would combine with an up (or down) antiquark to form a D^0 (or a D^+) and the charm antiquark would combine with an up (or down) quark to form a $\bar{D}^0$ (or a D^-). Thus the binding energy of the J/ψ is

$$\epsilon_{J/\psi} = m_{D\bar{D}} - m_{J/\psi} = 634MeV. \tag{1.18}$$

The combination of a large binding energy and small size makes the J/ψ hard to break apart. This topic will be explored more in the next section.

1.4.2 Properties of the Dilepton Decay Products of the J/ψ

The J/ψ has large branching ratios for decay into dileptons of 6% for both dielectrons and dimuons. This is important because the dileptons carry the information about the J/ψ in the form of their invariant mass, m_{inv}, which for a lepton pair is given by

$$m_{inv} = \sqrt{(E_1 + E_2)^2 - (\vec{p}_1 + \vec{p}_2)^2}. \tag{1.19}$$

Experimentalists make plots of the invariant masses of the dileptons to see the resonance particles, such as the J/ψ, as peaks in the spectrum. The peak is centered over the accepted mass for the resonance particle. The charged leptons only interact electromagnetically with the matter they pass through, so they can conceivably survive a trip through the high multiplicity environment of a nucleus-nucleus collision without interaction. That means the information they carry of their parent particle is intact. This allows our study of the initial state of the collision.

Even though the dileptons only interact electromagnetically, there are slight differences between how the electrons and muons interact with matter. The electrons do not penetrate through matter very far before an interaction, primarily through ionization, and are easily bumped off their path. The muons, on the other hand, are heavier and thus harder to bump off their path. They go almost straight through matter. Now, comparing this to hadrons trying to pass through matter, the hadrons interact strongly. This means that when a hadron enters matter, it pass through some distance and then break apart in a shower of particles, hadronic shower. With sufficient material, the signal to background ratio will be high for the muons, because the hadrons will be absorbed. This makes the dimuons an especially "clean" signal, and is the situation that experimentalists desire in a signal.

1.5 Why Another Event Generator?

The main reason for writing SPACY is to do a Monte Carlo full space-time development of a nucleus-nucleus collision. Most of the event generators that study J/ψ production, such as those by S. Gavin and R. Vogt [18], only solve an analytical model. This model is the Glauber model and it consists of a group of integrals to model a nucleus-nucleus collision through the nuclear geometry.

SPACY was written to consider only a hadronic scenario, so we assume a nucleus-nucleus collision is no more than an aggregate of independent nucleon-nucleon collisions. In these collisions, there are probabilties and cross sections, for particle production in p+p and p+n inelastic collisions, that are parameterized from experimental data. The algorithms and other assumptions of SPACY are explained in the SPACY section.

Another reason to write SPACY is that experimentalists like to have full control of the code of an event generator to be able to make the changes they desire. There are other event generators that make approximately the same Monte Carlo cascade code calculations that SPACY does, but we do not control those codes. In fact, there is a policy for the use of one of the event generators UrQMD [19], Ultrarelativistic Quantum Molecular Dynamics, that states that the authors must be informed and consent to any changes made to the code. If we have to go through the authors of the code for changes, then it may take longer than we desire and

the changes may not be approved for publication. However, if we write our own code, we control the physics going into it and these changes are instantaneous.

1.6 Goals of SPACY

SPACY was created to specifically study the interactions of a J/ψ meson with the other produced particles from a nucleus-nucleus collision. We will compare these results on the J/ψ production to the recent results of NA50, which include two separate results. The first is the "anomalous" suppression of the J/ψ [5] and an observation of a threshold effect in the suppression as a function of transverse energy [1]. Part of this thesis work involves understanding these results. Another goal of the thesis is a comparison of whether the hadronic scenario used in SPACY can explain these NA50 results or whether a partonic (QGP) explanation is necessary. This is important because NA50 claims that only a partonic scenario can explain their data [1]. Another reason is that SPACY was created to serve as an initial exercise in the creation of a Monte Carlo "cocktail" containing contributions from all sources of dileptons in a nucleus-nucleus collisions at RHIC. This is a necessary part of the data analysis process.

The next section explores the history of J/ψ suppression and production to describe where the field currently is in terms of experimental and theoretical progress. Section 3 is an overview of SPACY, how its output compares to experi-

mental data, and how it models J/ψ production. Section 4 compares the output of SPACY to the recent experimental results from experiment NA50 at the CERN SPS. Section 5 discusses conclusions concerning SPACY's effectiveness as a model.

Chapter 2

History of J/ψ Production and Suppression

The 1S bound state of the charm and anticharm quarks was discovered simultaneously in November 1974 at Brookhaven National Laboratory [20] and Stanford Linear Accelerator Center [21]. The group on the East Coast called this new particle the J particle and the West Coast group called it the ψ. Since the particle was discovered simultaneously, it was called the J/ψ meson. The subsequent higher states such as the $2S$ were called ψ' and the three $3P$ states were called the χ_{c0}, χ_{c1}, and χ_{c2}. (Often these three mesons cannot be resolved in experiments, so they are referred to collectively as χ_c.) Since its discovery, the J/ψ in particular has been studied in great detail over differing conditions of production. This chapter is a review of the history of the J/ψ as it relates to our studies of nucleus-nucleus

collisions.

2.1 Matsui and Satz's Proposal

In 1986, Matsui and Satz wrote a paper entitled "J/ψ Suppression by Quark-Gluon Plasma Formation" [16]. This paper was the first publication that predicted that color screening of a $c\bar{c}$ pair would be a signature of a plasma formation. This proposal instigated a large amount of theoretical and experimental work. In the 13 years since this initial prediction, there have been hundreds of papers published on this phenomenon.

2.1.1 Color Screening

It is predicted that in a quark-gluon plasma, there will be a screening of the quark color charge, thus preventing the formation of a J/ψ meson. The charm quark and antiquark will then head in separate directions and eventually bind with lighter quarks to form the open charm mesons (D, $\bar{D}$, etc.). This color charge screening is similar to the charge screening phenomenon in solid state physics, so it also shares the same name, Debye screening. After the J/ψ is formed it must make the journey through the nuclear medium. So, now the question is how tightly bound is the J/ψ meson, which is similar to determining the radius of the bound state, $r_{J/\psi}$.

It is estimated that $r_{J/\psi} \simeq 0.20$ fm [16]. However, if the temperature is in-

creased as one would expect in a quark-gluon plasma, then there will be more quarks that interact with the c and $\bar{c}$. These extra interactions change the potential between the $c\bar{c}$ pair, which can prevent formation of a bound state. This changed potential leads to a new minimum distance between the charm quark and antiquark for there still to be a charmonium meson formed. It is predicted that J/ψ production is prevented down to $T = 1.2\,T_c$, where T_c is the phase transition temperature [16].

2.1.2 Background Enhancement

There are other possible backgrounds that may mask a J/ψ suppression by giving a large contribution in the J/ψ region of the dilepton invariant mass spectrum. These processes include the Drell-Yan process and open charm, D meson, decay. The invariant mass of the Drell-Yan dileptons will be dominant in the region of the J/ψ peak and above, while the open charm decays are dominant in the region below the J/ψ peak. There, pions that decay to single muons may be combined with another muon to form a lower mass dimuon pair. This type of background is called combinatoric background. Also, if a QGP is formed then some more dileptons are expected from quark-antiquark annihilation, thermal dileptons. It is possible that these dileptons could be created in the same range as the J/ψ mass peak and thus mask a J/ψ suppression signal.

2.2 First SPS Experimental Results - NA38

Shortly after the 1986 prediction from Matsui and Satz [16], the experiment NA38 started taking data at the CERN SPS. They observed various p+A systems and A+B systems all the way up ^{32}S on a U target. They also studied pA collisions to study any systematic effects in the data.

The first signs of a J/ψ suppression were seen in AB collisions with ^{16}O as the projectile on a U target in 1986 [17]. These results are based on a ratio S, which is the ratio of the number of J/ψ mesons observed to the number of muons from the continuum (in the J/ψ mass region). NA38 ended their first publication by stating, "Although the J/ψ suppression has been predicted as a signature of QGP formation, it is not excluded that alternative mechanisms could explain, as least partly, our experimental results." [17]. One problem NA38 had is the background that occurs in the low mass region, which is flooded from opposite-sign muon pairs from π and K decays.

The suppression was also reportedly seen in S+U collisions [22]. This data was analyzed with a slightly different analysis method. It employed comparison of the J/ψ cross section to that of the Drell-Yan. Then, this ratio was compared to the product of the projectile and target mass numbers and the new variable, L. This variable L represents the amount of nuclear matter the J/ψ traverses on its journey out of the collision region. The Drell-Yan dileptons are used as a reference

process to J/ψ production because they are predicted to have no suppression in p+p, p+A, or A+B collisions.

2.3 Hadronic Absorption Mechanisms

2.3.1 Nuclear Absorption

Nuclear absorption of the J/ψ was first studied by C. Gerschel and J. Hüfner in 1988 [23]. They set out to find a common data analysis procedure for all experiments that measured J/ψ production. This was important because the different experiments used different projectiles on the nuclei in their targets. These projectiles include protons, antiprotons, pion, photons, and nuclei. Gerschel and Hüfner started with the assumption that a $c\bar{c}$ pair that will evolve into a J/ψ formed in the collision region is absorbed in the nuclear matter. Then, they analyzed the previous data as a function of the mean length of the path of the $c\bar{c}$ pair through the nuclei, L.

Gerschel and Hüfner, in a later paper [24], gave an extrapolation of the 1988 work that has become the standard equation to describe the cross-section of J/ψ, in this case, for p+A collisions. This equation is

$$\sigma_{pA} = A\sigma_{pN}\exp\left[-\rho_o\sigma_{\rm abs}^{\psi \rm N}{\rm L}\right], \tag{2.1}$$

where σ_{pA} is the cross section of production for $p + A \rightarrow J/\psi + X$, σ_{pN} is the J/ψ

production cross section on an individual nucleon, ρ_o is the nuclear matter density, $\sigma_{abs}^{\psi N}$ is the cross section for absorption of a J/ψ by a nucleon[1], and L is the effective length of the J/ψ's trajectory inside the target nucleus (for p+A collisions). The term $A\sigma_{pN}$ deals with the production of the J/ψ, while the term $\exp\left[-\rho_{\rm o}\sigma_{\rm abs}^{\psi \rm N}{\rm L}\right]$ represents the absorption. A common form to represent this equation is

$$\sigma_{pA} = A^{\alpha}\sigma_{pN}. \tag{2.2}$$

The exponent α represents the amount of suppression in the collision. For $\alpha = 1$, there is no J/ψ suppression compared to p+p collisions. An $\alpha < 1$, represents some absoprtion. A value for α was found by E772 and is discussed below. The main difference bewteen p+A and AB collisions in Eq. 2.2 is that A becomes an AB, accounting for the extra nuclear matter from a projectile nucleus. This also means that L has to be calculated differently because there is more nuclear matter for the J/ψ to pass through.

When various experimental data points for p+A collisions were plotted against this new variable L, the result was an absorption cross section of $\sigma_{abs}^{\psi N} = 6.2 \pm 0.3$mb [25]. This absorption cross section was independent of the energy of the collisions observed and independent of the projectiles, p, $\bar{p}$, π, and γ. For the nucleus-nucleus collisions, the absorption cross section was found to be $\sigma_{abs}^{\psi N} =$

[1] J/ψ is written interchangeably with ψ.

5.8 ± 1.8mb [25]. Comparisons of these various experimental results is valid, because they all were taken over approximately the same x_F range. Another point worth considering is that $\sigma_{abs}^{\psi N}$ is higher for both the single particle projectiles and the nuclear projectiles when compared to photoproduction results. The photoproduction results used for comparison were $\sigma_{abs}^{\psi N} = 3.5 \pm 0.8 \pm 0.5$mb [26]. This descrepancy is resolved by Gerschel and Hüfner [25] by noting that Anderson *et al* used only a one arm spectrometer that could not reconstruct the decay of a J/ψ from its decay products.

The main result of this work is that the projectile independence means that nuclear absorption is a final state effect. This absorption also describes the results from NA38's oxygen and sulpher beam results.

2.3.2 Hadronic Comovers

It was first proposed by S. Gavin, M. Gyulassy, and A. Jackson [27] and R. Vogt, M. Prakash, P. Koch, and T.H. Hansson [28] that J/ψ mesons would be suppressed through collisions with other produced hadrons, or comovers. This explanation is appealing because it allows a small nuclear absorption cross section like those from photoproduction experiments, but gives an additional absorption to bring the effective cross section for hadronic J/ψ suppression up to the $6 - 7$ mb value quoted by Gerschel and Hüfner and the NA38/NA50 experiment. The essence of the comover theory is shown in Fig. 2.1, which shows a J/ψ meson colliding with

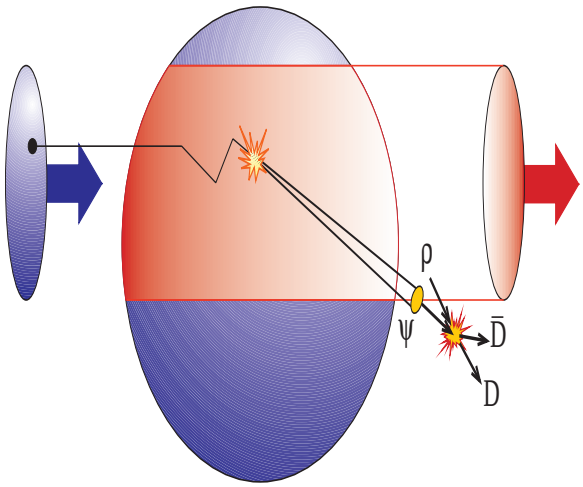

Figure 2.1: A J/ψ and ρ meson collision that gives an example of absorption by co-movers.

a ρ meson, the comover[2].

A measure of the J/ψ suppression is the survival probability, S, which is the percentage of J/ψ mesons that are created and survive their journey through the nuclear medium. For comover absorption, this survival probability, S_{co}, is predicted to be [18],

$$S_{co} = exp\left[-\sigma_{co} v_{rel} n_o \tau_o \ln R_T / v_{rel} \tau_o\right], \tag{2.3}$$

where σ_{co} is the cross section for a charmonium and comover interaction. The variable v_{rel} is the relative velocity between the charmonium and comover, n_o is the density of comovers, τ_o is the time in the charmonium's rest frame, and R_T

[2]This figure is reprinted with permission of S. Gavin.

is the transverse size of the collision region. If we scale up to an AB collision for the S+U and Pb+Pb collisions observed by NA50, then we have $S = S_A S_B S_{co}$, where $S_{A,B}$ is the survival probability from nucler absorption for nucleus A and B, respectively. This means that a J/ψ survives collisions with (or does not collide with) nucleons from nucleus A, nucleons from nucleus B, and the comovers.

Let us consider the feeddown from heavier charmonium mesons, the χ_c mesons contribute to $\sim 30\%$ of the observed J/ψ mesons and the ψ' contributes $\sim 12\%$. Thus, the comover survival probability should reflect this by weighting the various contibutions [29]

$$S_{co}(b,s) = 0.58 S_{\psi}(b,s) + 0.30 S_{\chi_c}(b,s) + 0.12 S_{\psi'}(b,s), \tag{2.4}$$

where b is a particular impact parameter and s is the meson's formation position. If we consider the possibility of a QGP formation, we have to consider suppression due to color screening. This is especially important for the heavier charmonia because they "melt" at a lower temperature than the J/ψ meson. So, now we have a modified S_{co} [29]

$$S_{co}(b,s) = 0.58 S_{\psi}^{co} S_{\psi}^{QGP} + 0.30 S_{\chi_c}^{co} S_{\chi_c}^{QGP} + 0.12 S_{\psi'}^{co} S_{\psi'}^{QGP}. \tag{2.5}$$

The earlier "melting" of the ψ' and χ_c mean that some of the observed suppression is actually this effect and not a phase transition.

2.4 Fermilab Results and the Theoretical Implications

In the early 1990s, two experiments at Fermilab provided important and theoretically interesting results concerning J/ψ production. The first results are ψ' and J/ψ high-p_T production results from CDF. The next results concerned the α values of J/ψ and ψ' mesons as measured in the E772 experiment. Later, refinement of these measurements was made by the same experiment with different names, E789 and E866.

2.4.1 CDF High p_T Results

The CDF measurements of the J/ψ provided valuable insight into its production mechanism because they measured $p + \bar{p}$ collisions, a more basic collision system. These results extended higher in p_T than previous experiments because the $\sqrt{s}$ was higher than for any previous experiments. The results for J/ψ and ψ' production cross sections are shown in Figs. 2.2 and Fig. 2.3, respectively.

These two plots show how the color singlet model fails to accurately predict the J/ψ and ψ' production rates. Historically, this shortfall of the color singlet model was first observed with the ψ' and was thus dubbed the "CDF ψ(2s) anomaly." The anomaly refers to the data exceeding the predicted rates by factors of 50! The solution to this problem was the consideration of another mode of production

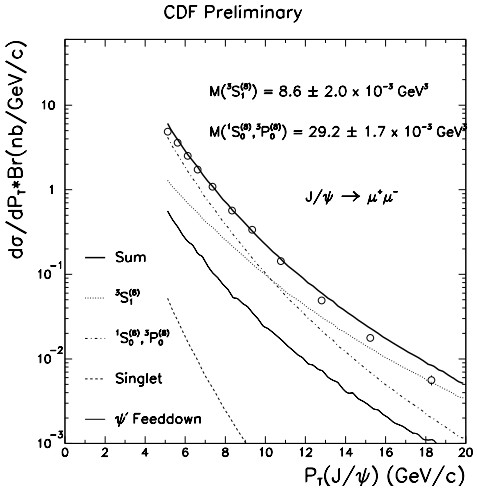

Figure 2.2: Production cross sections of the J/ψ vs. p_T of data and various production models [2]. The models with a superscript of (8) represent color octet production of that state.

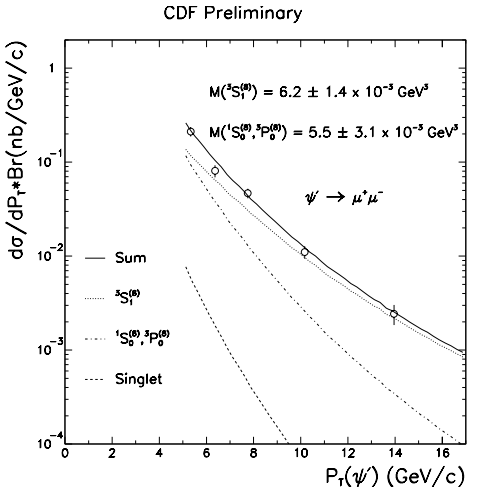

Figure 2.3: Production cross sections of the ψ' vs. p_T of data and various production models [2]. The models with a superscript of (8) represent color octet production of that state.

that supplements the color singlet production. This new mode was proposed by Braaten and Fleming [30] and is called the color octet model. This model along with feeddown contributions from the χ_c and ψ' mesons explain the CDF data.

2.4.2 Color-Octet vs. Color-Singlet

The theory of Fleming and Braaten proposed another formation mechanism for charmonium mesons. The $c\bar{c}$ pair is produced quickly, $\tau_o \simeq (2m_c) \simeq 0.07\,\mathrm{fm/c}$ [31]. It is produced in a colored state coupled with a gluon, $c\bar{c}g$. Charmonium is then formed by a color neutralization process that is not completely understood, but involves the loss of the extra gluon. This process occurs over a time of 0.3 fm/c, which is a long time for the color-octet to traverse the nuclear medium because the target nucleus is Lorentz contracted.

This color-octet mechanism supplements the color-singlet mechanism to explain the magnitude of the production at CDF. The color-singlet model predicts that the $c\bar{c}$ is formed in a color neutral state and later becomes the color-singlet J/ψ or other charmonium state. This model actually predicts that most of the J/ψ mesons come from feeddown of χ mesons. The color-singlet model predicts the χ contribution to be on the order of 90%, but CDF measured it to be approximately 30% [32]. This result also facilitated the need for the color-octet model to explain the data.

2.4.3 Fermilab Fixed-Target Results

A series of experiments carried out by the same collaboration which carried the names E772, E789, and E866 at Fermilab. This experiment measures high mass muon pairs in p+A collisions at $\sqrt{s} = 800$ GeV. One of the first results from E772 was that the α variable had a value for J/ψ production of 0.92, confirming nuclear suppression (an $\alpha < 1$) [3]. The plot is shown in Figure 2.4. The α variable comes from the equation for the nuclear dependence of J/ψ production

$$\sigma_{pA} = A^{\alpha}\sigma_{pp}. \tag{2.6}$$

Another result is that as α increases, suppression decreases. For $\alpha = 1$, there is no suppression. For $\alpha > 1$, there is an enhancement. For $\alpha < 1$, there is an absorption.

This plot also shows that the J/ψ and ψ' have approximately the same absorption [3]. One could conclude that at some point in the production they have the same interaction cross section, which means that some preresonance state exists that has the same cross section regardless of the charmonium state it becomes later.

The latest results from E866 show the x_F dependence for the α values of J/ψ and ψ' mesons. The x_F variable is defined as $x_F = \frac{p_z}{p_{z,max}}$, where $p_{z,max} \simeq \frac{1}{2}\sqrt{s}$. The x_F variable is a measure of the forward momentum that the J/ψ possesses.

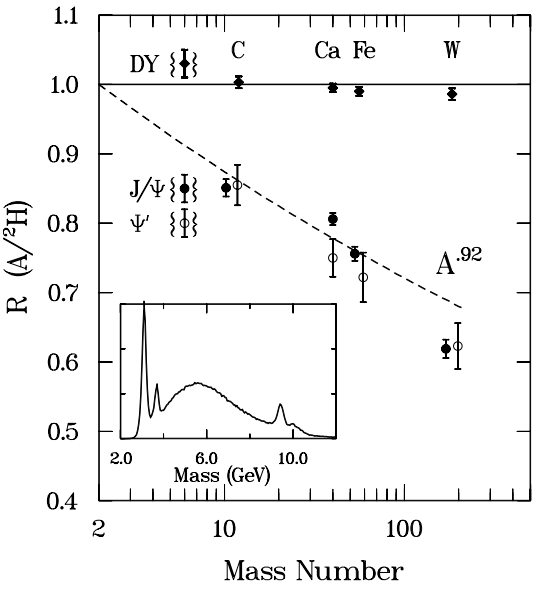

Figure 2.4: Ratios of cross sections of nuclei to deuterium verses mass number, A [3].

The results show that with increasing x_F, the alpha decreases for the J/ψ and ψ'. The results are shown in Fig. 2.5[3]

2.5 Preresonance Absorption

There is a need to explain how both the ψ' and J/ψ have comparable absorption cross sections, especially since the ψ' is so much larger than the J/ψ and would be expected to have a larger absorption cross section. It is natural to conclude that having the same absorption cross section could mean they had a common size at some point. It is predicted that the $c\bar{c}$ pair is formed in a single preresonance,

[3]These preliminary results are courtesy of Mike Leitch, the E866 spokesman.

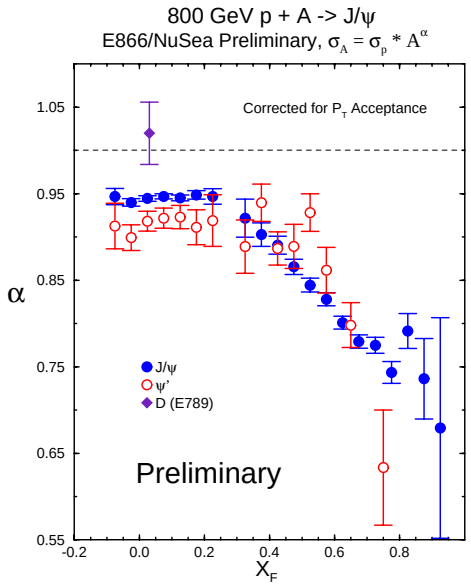

Figure 2.5: Preliminary α values versus x_F [4].

or precursor, state that may or may not be the color-octet state. The important features of this model are that the precursor lives for a short amount of time (approximately the same as the color octet, 0.3 fm/c) and has a large cross section for absorption in the collision region. This partonic absorption in the very early stages of the collision should not be confused with the formation of a QGP.

2.6 Latest SPS Experimental Results - NA50

There have been two papers published in the last three years by the NA50 collaboration that have possibly important implications. The first result describes the anomalous suppression in Pb+Pb collisions [5] and the second discusses a possible

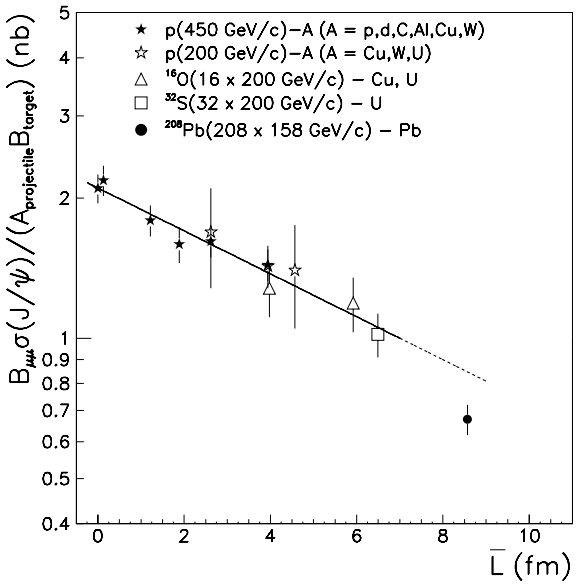

Figure 2.6: Cross section of J/ψ divided by AB versus L [5].

threshold effect in the E_T distribution [1].

2.6.1 "Anomalous" Suppression

The final analysis of the 1995 data showed a very intriguing result [5], "anomalous" suppression of the J/ψ. This suppression was observed in central Pb+Pb collisions and can be observed in a plot of the cross section of the J/ψ (times the branching ratio of J/ψ to $\mu^+\mu^-$ and divided by AB) versus the L variable that was proposed by Gerschel and Hüfner [25] (Fig. 2.6).

Another run in 1996 had better capabilities to analyze peripheral events and collected more statistics for central collisions. The 1996 data show that the central collisions are the only ones with suppression, whereas the peripheral events fall

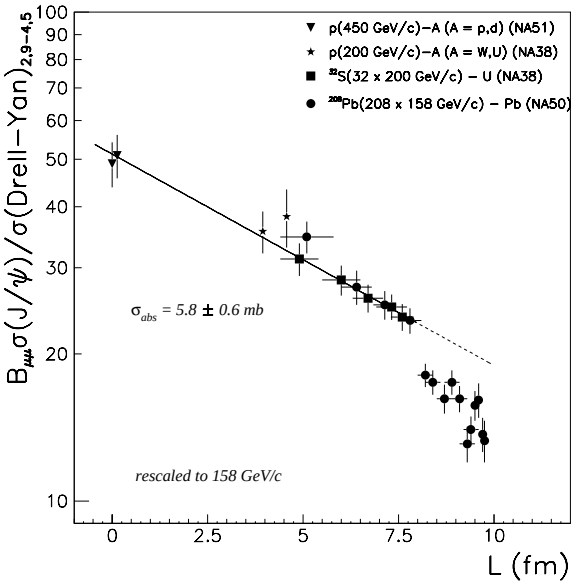

Figure 2.7: Ratio of the cross sections of J/ψ to Drell-Yan versus L with the 1996 data [6].

on the nuclear suppression line, see Fig. 2.7. Thus, one can conclude that there must be something else happening besides the expected suppression in the Pb+Pb collisions.

Another result from NA50 is a measurement on ψ' production. The ψ''s larger radius suggests that it would suffer suppression sooner than the J/ψ. There is an observed anomalous suppression already in S+U collisions for the ψ'. This behavior is demonstrated in Fig. 2.8.

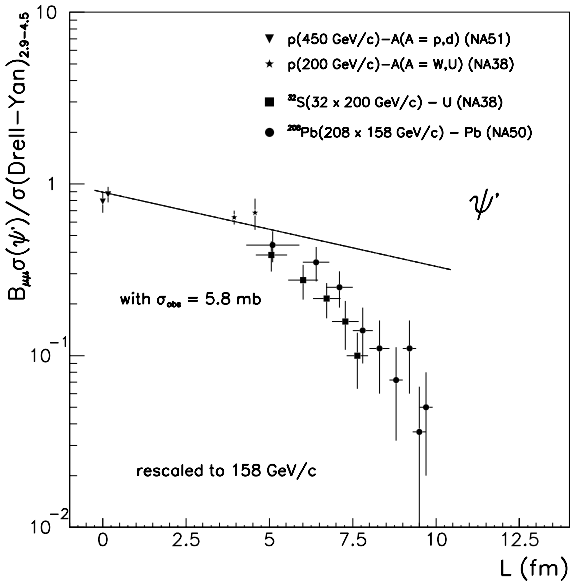

Figure 2.8: Ratio of the cross sections of ψ' to Drell-Yan versus L [6].

2.6.2 E_T Dependence of the Suppression

The 1996 data taking period for NA50 was a high statistics run to test their results on anomalous suppression based on the 1995 data. Besides the confirmation of anomalous suppression, an observation of a threshold in the E_T dependence of ratio of the J/ψ cross section to that of the Drell-Yan dileptons holds very interesting implications [5]. A threshold could mean that a phase transition has occurred to the QGP and more suppression is occuring due to color screening. These results are shown in Figure 2.9. The validity of the results was questioned because of the method in obtaining the cross section of the Drell-Yan distribution. So, NA50 reanalyzed the results with shifted bins in E_T to show that the threshold

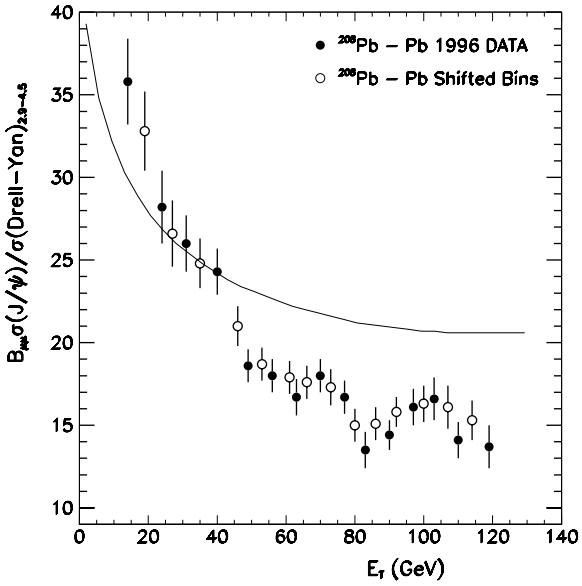

Figure 2.9: Ratio of the cross sections of J/ψ to Drell-Yan as a function of transverse energy [1]. The curve represents expectations from nuclear absorption.

was not an artifact of the binning. These shifted bins are also shown in Figure 2.9. There was still concern about the validity of the data analysis technique. So, they recalculated the Drell-Yan using the minimum bias E_T distribution to obtain the Drell-Yan data. These results are shown in Figure 2.10. This method of analysis is based on the Drell-Yan and minimum bias data being overlayed. Then, the minimum bias distribution's tail provides the function to provide a smooth fit to the Drell-Yan data. Basically, the minimum bias is used to fit the Drell-Yan and avoid the statistical fluctuations in the Drell-Yan distribution.

The reanalysis with the minimum bias events gives the same behavior as the results that used Drell-Yan, which reinforces the validity of the results. More

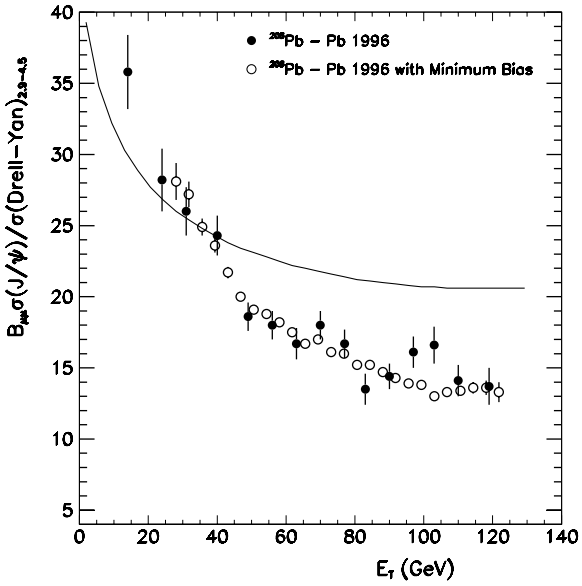

Figure 2.10: Comparison of the ratios of the cross sections of J/ψ to Drell-Yan (from Drell-Yan events) and J/ψ to Drell-Yan (from minimum bias events) as a function of transverse energy [1]. The solid curve represents expected nuclear absorption.

discussion of these results will occur in the Discussion and Summary sections below.

2.7 Current Theoretical Explanations

There are many attempts by theorists to explain the latest NA50 results. Some of these attempts will be discussed below. I will attempt to describe a few of the theories in current use. However, for a complete review of these theories and more, please refer to the proceedings of the recent INT/RHIC workshop "Charmonium Production in Relativistic Nuclear Collisions" [33], Quark Matter '97 [34], and

Quark Matter '99 [35].

2.7.1 A New Phase of Matter?

One theory proposed to explain the NA50 results is that there is a change in the phase of matter in the collision region of the Pb+Pb collisions at the CERN SPS. The main driving force behind this theory is that nuclear absorption cannot explain the suppression. Also, there are not enough energetic comovers to bring the suppression into agreement with the data. This extra suppression may mean that something else is happening. This extra suppression might indicate the formation of a quark-gluon plasma as predicted by Matsui and Satz [16].

2.7.2 Hard Gluons

The comover absorption theory may not need to be invoked if high momentum gluons are responsible for any extra absorption beyond nuclear absorption. The produced hadrons may not have enough energy to overcome the threshold energy of many of the reactions [36]. However, hard gluons created in the collision can easily break apart a J/ψ meson.

Now, the question that must be answered is how many of these hard gluons are produced and at what energies. Hüfner and Kopeliovich have recently explored an additional suppression mechanism to nuclear absorption in the form of gluons. This is needed to account for the discrepancy between the absorption cross section

from p+A data, $\sigma_{abs} \simeq 6 - 7$mb and the photoproduction results analyzed with a coupled-channel analysis, $\sigma_{abs} \simeq 3 - 4$mb [37].

The basis of their model is that charmonium doesn't just interact with undisturbed nucleons (N) as in nuclear absorption model but can also interact with disturbed nucleons (N^*) and the debris from the nucleon-nucleon interaction, which are gluons. The interaction for charmonium with these disturbed or "wounded" nucleons is normal nucleon interaction plus gluon interaction [37]

$$\sigma_{abs}(\Psi N^*) = \sigma_{abs}(\Psi N) + \sigma_{abs}(\Psi g)\langle n_g \rangle, \tag{2.7}$$

where Ψ is either a J/ψ or ψ' and $< n_g >$ is the mean number of gluons radiated in a NN interaction preceeding the interaction with the charmonium. Using this new absorption, the term for the survival probability of charmonium in an AB collision is quite complex and I will not reproduce it here. The main result though is that the effect of hard gluons will decrease at RHIC and even more so at the LHC. The other important factor to consider is $\sigma_{abs}(J/\psi g)$, which is predicted to be about $\frac{3}{4}\sigma_{abs}(J/\psi N))$ [37]. This gives $\sigma_{abs}(J/\psi g) \simeq 3$mb. This value combined with the predictions for $< n_g >$ give a fit to the NA50 Pb+Pb and S+U data. The authors [37] point out that gluons will contribute less at RHIC due to the formation time effect. But, they also state that the comover interactions will increase, because of the increase in energy.

2.7.3 Comovers

It was shown by Gavin and Vogt [18] that a conventional comover model cannot explain the NA50 results. Recent work by Cassing *et al* has predicted that comoving strings of "prehadrons" could cause most of the dissociation of J/ψ mesons. They use a cascade code to evaluate the possible dissociation of J/ψ mesons with hadronic comovers instead of using a Glauber (analytical) model as Gavin and Vogt did. Cassing *et al*'s main comover suppression does not come from produced hadrons but "prehadrons." These are the strings in a collision that will become hadrons but have not yet reached the formation time to become a hadron. These strings are responsible for most of the suppression of the J/ψ by breaking it apart before it has had time to form, leaving fewer J/ψ's to be suppressed by hadronic comovers. This early suppression occurs before 0.8 fm/c [38]. They claim that the inclusion of strings can describe the p+A, NA38, and NA50 results on J/ψ suppression.

To summarize, there are three schools of thought on how to explain the NA50 data. The first is those who predict a completely partonic scenario, formation of a quark-gluon plasma. A second suggests a combined hadronic and partonic scenario to explain the data. Then, there is the possibility that everything can be accomodated in a completely hadronic scenario. More experimental data are needed to resolve this question.

Chapter 3

SPACY

SPACY [39] is a FORTRAN based computer code that carries out calculations in a Monte Carlo cascade framework to study the space-time development of a nucleus-nucleus collision. SPACY is based on a previous code that studied energy density in these collisions, ODIN [40]. This chapter will describe the basic physics assumptions and formulas used for the different processes in the various collisions in an event, which is a p+p, p+A, or A+B collision. It will also discuss how the vector meson production was modeled.

3.1 General Overview

A general Monte Carlo computer code is a program that uses random numbers selected from a probability distribution to simulate desired or predicted distributions. SPACY uses this method to characterize each binary collision and model

the outcome of the collision. A general cascade code is one that allows scattering of a particle and any created particles to scatter with other particles. A good example of this would be a program that tracked all the particles in a nuclear fission chain reaction. SPACY follows the space-time development of the particles in the original nuclei and those that are created, until all collisions have occurred. The order in which these collisions occur is frame dependent so we choose the nucleon-nucleon center of momentum (or center of mass) frame for the time ordering of collisions.

The motivation for this type of computer intensive event generator was discussed in Chapters 1 and 2. There are many unknown factors about the comover model that may or may not allow a hadronic explanation to the threshold behavior of J/ψ suppression as observed by the NA50 collaboration [1]. This knowledge will also be important to future experiments at the Relativistic Heavy Ion Collider (RHIC). SPACY attempts to address these questions by using a Monte Carlo code and not an analytical model.

Let us consider the general flow of SPACY. First, the nucleons are chosen at positions given by a nuclear density distribution (which can be spherical or deformed) and set into motion. Next, possible binary (two-particle) collisions are calculated and the first collision is chosen and calculated. As the first collision is carried out, SPACY starts the "clock" (t=0 fm/c). The type of collision, elastic or inelastic, is determined from the relevant cross sections. The new trajectories

of the particles scattered or created are calculated and their next collisions are calculated. Then, the next binary collision is found and calculated in the same manner as the first collision. These processes will be discussed in detail in the sections below.

3.2 Physics Assumptions

There are only two basic physics assumptions SPACY uses to study nucleus-nucleus collisions. One of the assumptions is that there is no new parton-level physics in nucleus-nucleus collisions. We do not simulate a quark-gluon plasma formation and only consider a purely hadronic scenario. At all times, we consider all particles to be hadrons in all collisions. That means there are no partonic sources of J/ψ suppression included in SPACY. However, SPACY is written in such a way as to allow the insertion of partons into the calculations if desired at a later date. This could be used in the future to explore partonic and hadronic (but non QGP) explanations of the NA50 results.

The other assumption is that SPACY calculates one binary collision at a time, which means that a nucleus-nucleus collision is an aggregate of non-coherent binary collisions. These collisions consist of nucleon-nucleon, nucleon-meson, and meson-meson collisions. This does neglect nuclear effects such as nuclear shadowing, which is a change of the parton distributions (structure functions) of the

nucleons inside the nucleus.

3.3 Important Algorithms

SPACY's calculations of the various collisions in the cascade rely heavily on Lorentz transformations between three different frames. One of these frames is the Lab system, which is the reference frame that the particle detectors are in when they observe an event. Another frame is the nucleon-nucleon center of mass (NN frame), which is the center of momentum frame of the projectile and target nucleons. The NN and Lab frames are the same for a collider event. The third frame is called the Local frame and it is the center of momentum of the two colliding particles in a binary collision. The local frame is used to determine if a collision is elastic or inelastic.

When SPACY calculates a nucleus-nucleus event, the first subroutine carried out is the creation of the nuclei. SPACY has been constructed with a special emphasis on calculating the nuclear geometry correctly. It creates a nucleus by positioning the independent nucleons in a certain region that follows the density distribution for either speherical or deformed nuclei. We consider all nuclei with $8 \leq A \leq 19$ to be spherical with a Maxwellian radial probability distribution. For spherical nuclei with $A \geq 20$, the radial probability distribution is given by a Woods-Saxon distribution. In practice, the first Z number of nucleons are protons

and are placed according the distribution. The next A-Z nucleons are neutrons that are also placed according the distribution. To avoid overlapping nucleons, no nucleon is allowed to be placed closer than 0.5 fm to any previously generated nucleon. For deformed nuclei, the process is the same for sperical nuclei with $A \geq 20$ except that there is a non-zero deformation coefficient in the Woods-Saxon distribution. There is also an added angular dependence in the density distribution.

Before the nuclei are put into motion towards each other, SPACY optionally gives the nucleons Fermi motion. This is momentum with the nucleus relative to the other nucleons. The amount of momentum is given by the Thomas-Fermi approximation,

$$p(\vec{r}) = p_F \left[\frac{\rho(\vec{r})}{\rho(\vec{0})} \, u \right]^{1/3}, \tag{3.1}$$

where $p_F = 0.260\,\mathrm{GeV/c}$ and u is a random number in the closed interval $[0, 1]$. This distribution is assumed to be isotropic. SPACY checks this by disallowing any spurious center-of-mass motion.

SPACY also sets the impact parameter, b, between the two nuclei before they are set in motion. The value of b is chosen randomly by the equation

$$b = \sqrt{(b_{max}^2 - b_{min}^2)u + b_{min}^2}, \tag{3.2}$$

where b_{max} and b_{min} are read into SPACY from an input file that is created with

values set at the user's discretion. Typically, the value of b_{min} is 0 fm and b_{max} is the sum of the radii of the nuclei for a minimum bias collision. For a central collision, typically b_{min} is 0 fm and b_{max} is a small value, 0.1 fm for example. The variable u is a new random number in the interval $[0, 1]$. Then, SPACY checks if there will be any binary collisions at this impact parameter. It tries to find an i and j that represent nucleons in first and second nuclei, repectively, that satisfy

$$\pi[(r_{i,1} - r_{j,1} + b)^2 + (r_{i,2} - r_{j,2})^2] \leq \sigma_{NN}, \tag{3.3}$$

where r_1 and r_2 refer to the x and y components of nucleons i and j. The cross section, σ_{NN}, is the nucleon-nucleon scattering cross section. If SPACY's choice of b fails to produce any primary binary collisions, then it picks a new one until this condition in eq. 3.3 is satisfied.

The final item SPACY performs before starting an event is to Lorentz transform into the NN System. Then SPACY moves the nuclei to where the first primary binary collision where occur at $z = 0$. When this is completed, SPACY sends the nuclei in motion and carries out the first collision. This first collision also starts SPACY's clock at $t = 0$. The time ordering of collisions is frame dependent, so it is always carried out in the same frame, the center of momentum frame for the two nuclei (or projectile and target).

SPACY finds all possible binary collisions, which satisfy condition

$$d_{min} < \sqrt{\sigma/\pi}, \tag{3.4}$$

where d_{min} is the distance of closest approach for the particles. Then, SPACY fills a collision list with all these possible collisions and time orders them. The collision with the smallest amount of time until it occurs is carried out next. After a collision, this entire process is repeated because of new directions or particles from the collision process. Any collisions that now may not occur are removed from the list.

SPACY carries out binary collisions by transforming to the center of momentum frame of the two particles. Then, SPACY looks at the following condition to determine what type of collision to calculate,

$$u < \frac{\sigma_e(E_{12})}{\sigma_t(E_{12})}. \tag{3.5}$$

In this equation, u is a random number from the interval $[0, 1]$, $\sigma_e(E_{12})$ is the elastic scattering cross section at energy E_{12} (where E_{12} is the center of mass energy for particles 1 and 2, $E_{12} = E_1 + E_2$, also known as $\sqrt{s}$), and $\sigma_t(E_{12})$ is the total scattering cross section at energy E_{12}. If this condition is satisfied, then an elastic collision is calculated. In an elastic collision, the final particles are the same as the initial but they have received a small amount of p_T. This results in

new directions and future collisions for the particles.

If the elastic collision condition is not met, then an inelastic collision occurs. The original particles that participate in the binary collision have some rapidity loss that is reflected in a change in their p_z. A parameter, α, is used to characterize the inelasticity (or nuclear stopping power) of the collision. In SPACY, we use $\alpha = 1$, which is the value of the free nucleon-nucleon collisions. This value for α corresponds to an average inelasticity of 0.5, e.g. half of the available energy will be converted from kinetic energy of the colliding particles to energy carried by the newly created particles. The excess in energy, E_x, in the collision is given by

$$E_x = E_{12} - E'_{12}, \tag{3.6}$$

where E_{12} is the center of mass energy before the collision, and E'_{12} is the center of mass energy after the collision. E'_{12} is calculated by obtaining the E' and p'_z from the longitudinal momentum loss (defined below), obtaining p'_x and p'_y from the p'_T, and then using the equation

$$E'_{12} = \sqrt{(E')^2 - (\vec{p'})^2}. \tag{3.7}$$

If $E_x \geq 0$, then it possible to produce particles such as pions, kaons, or vector mesons. The algorithm for pion production is the same for kaon production but it will be described for pions. The vector meson production algorithm is described

in the next section.

The pions are produced randomly but constrained to fit certain distributions in transverse momentum and rapidity. The transverse momentum distribution is given in terms of a variable m. This relation is

$$m = m_T - m_\pi, \tag{3.8}$$

where m_T is the transverse mass which is $m_T = \sqrt{p_T^2 + m_\pi}$. The cross section's distribution with respect to m is

$$\frac{d\sigma}{dm} \sim \frac{m}{T_m} \exp\left(-\frac{\mathrm{m}}{\mathrm{T_m}}\right), \tag{3.9}$$

where T_m is a slope parameter that can be parameterized by $T_m(GeV) = 0.13GeV + 0.018(\log(E_{12}))$. The two colliding particles have original rapidities y_1 and y_2 and final rapidities y_1' and y_2'. The rapidity distribution is given by

$$\frac{d\sigma}{dy} \sim \left[(1 - x_1)(1 - x_2)\right]^a, \tag{3.10}$$

where $x_{1,2}$ is the minimum value of the numbers between 1 and $\frac{m_T}{m_{1,2}} \exp(\mathrm{y_2 - y_1})$ and a is parameter set in SPACY's input file that obeys the equation

$$a = 3.5 + 0.9 \log E_{12}. \tag{3.11}$$

The variable x is related to the rapidity y of the particle. The equation for x is

$$x = \frac{E' + p'_z}{E + p_z}, \tag{3.12}$$

where the primed variables represent the final state and the unprimed variables represent the initial state (before the collision). The rapidity used in Eqn. 3.10 is that of the final state given by

$$y = \frac{1}{2}\ln\left(\frac{\mathrm{E'} + \mathrm{p'_z}}{\mathrm{E'} - \mathrm{p'_z}}\right). \tag{3.13}$$

The angular distribution is randomized so a final particle's angle is $\phi = 2\pi u$, where u is the random number in the interval [0,1]. SPACY also ensures that energy and momentum is conserved in each binary collision before transforming back to the nuclear center of momentum frame. This is done in an iterative process, where the momentum and energy are adjusted until conservation is achieved to the level of 10^{-6} for both quantities.

There is also an option for the formation time of the pions which is important to the study of the comovers. This importance comes from the assumption in SPACY that the pions cannot rescatter with any particle before it reaches the formation time, τ_o, in its own rest frame. Before this time, it is assumed to be gluon field moving through the medium without interaction. When the pion comes on mass shell, it is only then allowed to scatter.

3.4 Model of J/ψ Production and Absorption

The model for J/ψ production and absorption follows a generally accepted model: a $c\bar{c}$ pair is created immediately after a binary collision in a precursor state that may or may not be a color-octet state. The main properties of the precursor are a relatively high cross section for interaction and short lifetime compared to the charmonium state to which it decays. The precursor's interaction is independent of whether it later decays to a J/ψ, ψ', or any of the three χ states.

The precursor is implemented in the following manner. From t=0 for the charmonium existence, the cross section for interaction with nucleons is that of the precursor. As soon as $t = \tau_{VM}$, the formation time of the charmonium state, then the cross section immediately switches to that of the charmonium formed. It can be represented as

$$\sigma_{charmonium} = \sigma_{octet}\theta(\tau_{VM} - t) + \sigma_{singlet}\theta(t - \tau_{VM}), \tag{3.14}$$

where σ_{octet} is the precursor's cross section for interaction and $\sigma_{singlet}$ is the charmonium's physical state cross section for interaction with nucleons, and θ is the step function. The J/ψ and ψ' have different cross sections for interaction. Considering the situation after the charmonium is formed is complicated by the presence of the comovers.

In order to calculate the rates of production and the distributions for vector

meson production, we used R. Vogt's calculations from the 1992 report, "Rate Estimates for Vector Mesons and Drell-Yan production in Relativistic Heavy Ion Collisions" [41]. From this report, we get a general rapidity distribution of the cross sections given by

$$B_{VM}\frac{d\sigma}{dy}\bigg|_{y=0} = A_{VM}\exp(-C_{VM}\tau), \tag{3.15}$$

where B_{VM} is the branching ratio for decay to muon pairs and A_{VM} is a normalization constant [41]. The variable τ is given by $\tau = M_{VM}/\sqrt{s}$, where M_{VM} represents the mass of the vector meson or Drell-Yan lepton pair. For the J/ψ, we have from previous data that [42]

$$A_{J/\psi} = 5\,\mathrm{x}\,10^{-32}\mathrm{cm}^2 = 5\,\mathrm{x}\,10^{-5}\mathrm{mb} \tag{3.16}$$

and

$$C_{J/\psi} = 14.7. \tag{3.17}$$

If the above equation is integrated, we obtain $B\sigma_{J/\psi} = 3.44\,\mathrm{x}\,10^{-6}$mb. From this, we can find the probability that a J/ψ meson is created in a p+p collision that decays to a $\mu^+\mu^-$ pair. Since the total p+p cross section is 40 mb, we get

$$B_{J/\psi\to\mu\mu}P_{J/\psi} = \frac{3.44\mathrm{x}10^{-6}\mathrm{mb}}{40\mathrm{mb}} = 8.6\mathrm{x}10^{-8}. \tag{3.18}$$

Using the same method for the ψ', we get $B_{\psi' \to \mu\mu} P_{\psi'} = 1.55 \,\mathrm{x}\, 10^{-9}$. That means only once in every 11.5 million events will a J/ψ be formed that decays to dimuons and only once in every 645 million events will a ψ' be formed that decays into a dimuon pair.

These very low probabilities for production are bad from the standpoint of the large amount of CPU time that would be required to accumulate decent statistics. So, SPACY uses a parameter that redefines the probability of J/ψ production per collision. This probability is set to $\mathrm{AB}^{-0.4}$, which is one for p+p collisions and 10^{-2} for Pb+Pb collisions. This factor increases the number of J/ψ and ψ' mesons produced but not by so much that the nuclear medium seen by the J/ψ is dramatically different than in reality. We looked for the smallest perturbation to this environment possible while decreasing the required CPU time to acquire adequate statistics for our study.

3.5 Calibration of Proton-Proton Collisions

Since the primary binary collisions of a nucleus-nucleus collision are considered to be independent, we use p+p experimental data to calibrate them. The p+p data is for free space or independent collisions, which have been extensively studied at a variety of energies. Using this data ensures that within the SPACY model the global environment of the collision region is being modelled correctly.

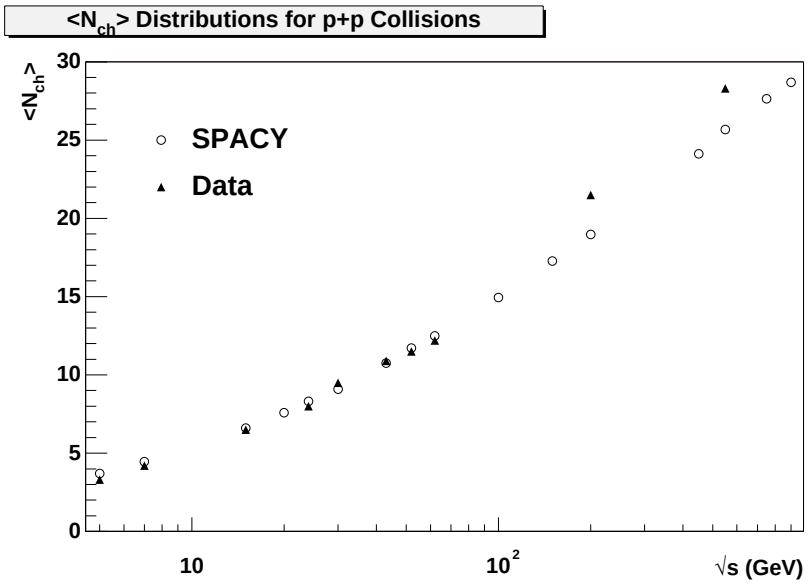

Figure 3.1: Mean charged particle multiplicity versus center of mass energies for SPACY predictions and experimental data.

Let us consider the mean charged particle multiplicity, $\langle N_{ch} \rangle$. From the Particle Data Book [7], we obtained data for p+p collisions at various values for $\sqrt{s}$. SPACY simulated 10,000 p+p collisions at various $\sqrt{s}$ values. The experimental data and the SPACY results for $\langle N_{ch} \rangle$ are shown in Table 3.1. These values are plotted against the experimental data in Figure 3.1. From this plot, we see that for $\sqrt{s} < 200$ GeV, SPACY has good agreement with the experimental data. For values greater than 200 GeV, SPACY's predictions deviate from the experimental results. However, NA50's Pb+Pb data was taken at a $\sqrt{s} \simeq 20$ GeV, where SPACY correctly predicts $\langle N_{ch} \rangle$.

Next, we consider the angular distibution of the particles by measuring the

Table 3.1: Table of SPACY predictions and experimental data for p+p collisions at various center of mass energies.

$\sqrt{s}$(GeV)	SPACY$\langle N_{ch}\rangle$	Experimental$\langle N_{ch}\rangle$
5.0	3.69	3.3
7.0	4.46	4.2
15.0	6.60	6.5
20.0	7.58	
24.0	8.30	8.0
30.0	9.08	9.5
43.0	10.75	10.9
52.0	11.71	11.5
62.0	12.49	12.2
100.0	14.94	
150.0	17.27	
200.0	18.97	21.5
450.0	24.12	
550.0	25.67	28.3
750.0	27.64	
900.0	28.68	35.5

pseudorapidity, η, distribution of the produced charged particles. The experimental data was obtained from the Particle Data Book [7], which reports only the positive values of η. So we assume these data points are symmetric with the negative values. We chose to simulate 10,000 p+p collisions at $\sqrt{s} = 53\,\mathrm{GeV}$ to compare SPACY to the experimental results (Figure 3.2). We see that SPACY's data is consistent with the experimental data in terms of magnitude and width of the distribution. Even though SPACY could not perfectly reproduce the distribution at midrapidity, we accept the parameters as acceptable. The peaks at $\eta > 4$ are the original protons after having interacted with each other. To compare the distributions, the SPACY data had to be event normalized, which means the number of counts over all the events is divided by the number of events.

A third variable to consider is the transverse momentum distribution of the particles. Since the majority of the produced particles are pions, we will look that their p_T distribution. The general form of the expected thermal distribution is

$$\frac{dN}{dp_T} = C p_T \exp\left(-p_T/T\right), \tag{3.19}$$

where C is some constant and T is the inverse slope of the p_T distribution. For pions, we expect that $T \approx 200\mathrm{MeV}$. From SPACY, the slope was fitted to be $T = 237\,\mathrm{MeV}$. A p_T distribution is shown in Figure 3.3. This plot is normalized so the y-axis is the probability of a particle having that p_T.

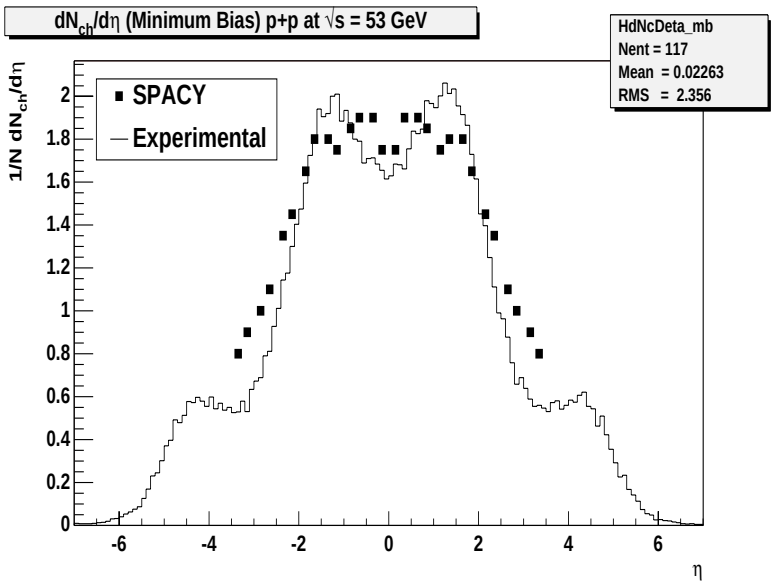

Figure 3.2: Pseudorapidity distribution to compare SPACY's prediction to experimental data from the Particle Data Book [7].

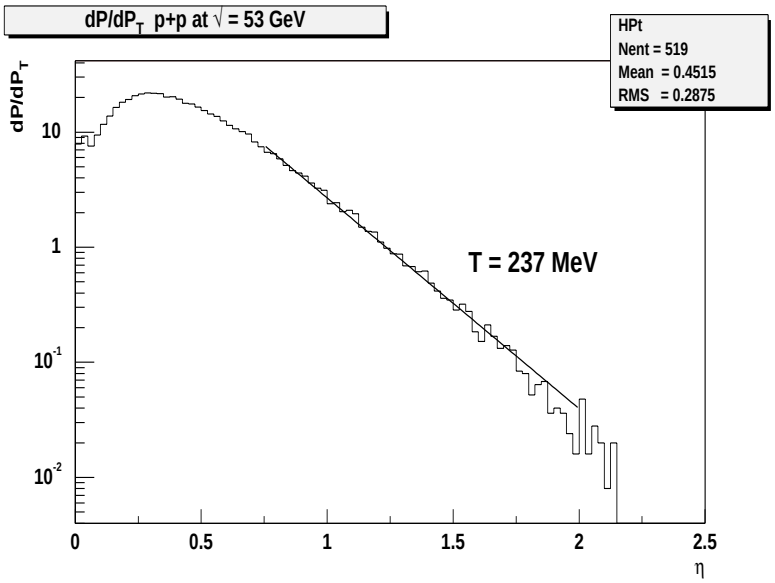

Figure 3.3: Transverse momentum distribution showing a fit to obtain the inverse slope value.

Now that the parameters are set and SPACY can correctly describe p+p collisions, we can continue onwards in our study of J/ψ suppression in nucleus-nucleus collisions.

3.6 Transverse Energy Distribution

The most recent published results from NA50 are an observation of a threshold in the E_T distribution of the ratio of the J/ψ cross section to the Drell-Yan cross section. Thus, we consider SPACY's predictions for the transverse energy distributions, especially for Pb+Pb collisions. We chose to compare SPACY's predictions to experimental data from the NA49 [43] and WA98 [44] experiments in addition to NA50 [45]. The reason for choosing these two experiments is that their calorimeter acceptances complement NA50's acceptance. NA50's acceptance is $1.1 < \eta < 2.3$, NA49's acceptance is $2.1 < \eta < 3.4$, and WA98's acceptance is $3.5 < \eta < 5.5$.

SPACY's predictions for the minimum bias E_T show excellent agreement with the data from WA98 (Figure 3.4) and NA49 (Figure 3.5). However, there is not as good agreement with the NA50 distribution (Figure 3.6), until we increased the SPACY values by 75% to match the 1995 NA50 data reported in [45]. This is not too surprising, since NA50 has only an electromagnetic and can only measure neutral transverse energy . This means that they can measure only the transverse

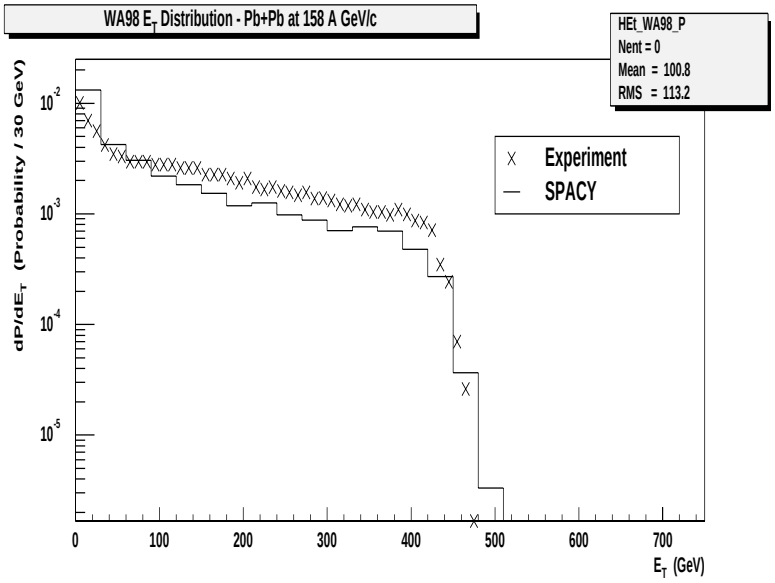

Figure 3.4: Minimum bias E_T distribution of SPACY data and experimental data from experiment NA50 in their acceptance.

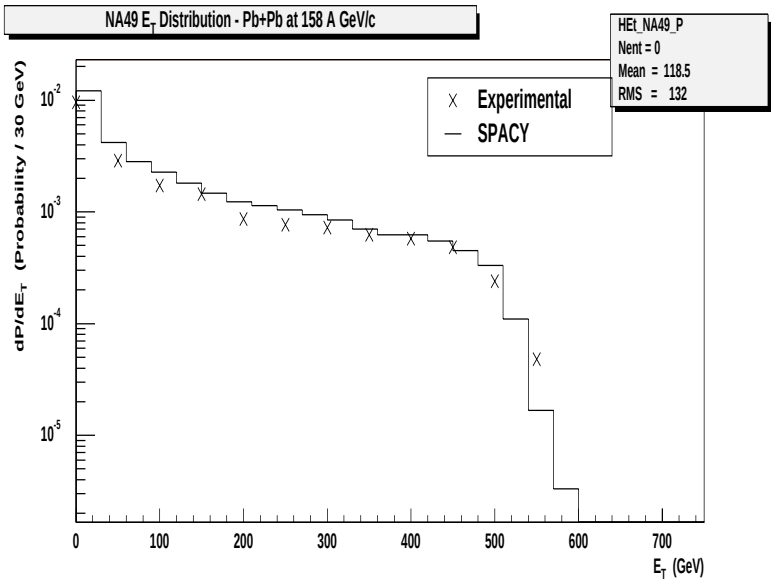

Figure 3.5: Minimum bias E_T distribution of SPACY data only in the NA49 acceptance.

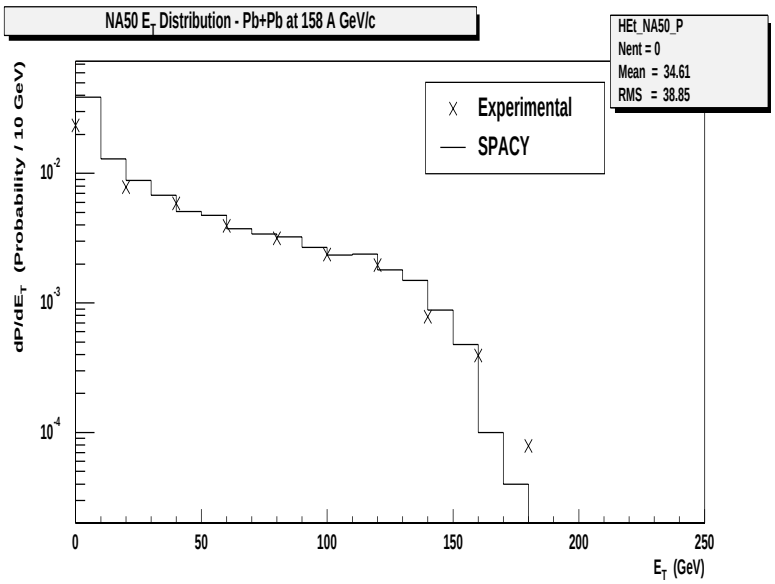

Figure 3.6: Minimum bias E_T distribution of SPACY data only in the NA50 acceptance.

energy of photons and π^o mesons (which decay to two photons). Thus, they need to scale their data to obtain the full transverse energy. The NA50 experiment also reported in [1] a correction factor to the scale factor, from neutral transverse energy to full transverse energy, of 74%. We found that the correction factor used to correct the SPACY data is consistent with the NA50 value (difference of 1%). Hence, we believe that SPACY correctly models the transverse energy production in the angular ranges of WA98, NA49, and NA50.

Chapter 4

Discussion of J/ψ Analysis

This chapter covers the analysis of the calculations made by SPACY about J/ψ production and suppression. As shown in the previous section, the p+p collisions without any charmonium production correctly create the hadronic environment the J/ψ mesons traverse. We will consider the process used to parameterize the preresonance state's lifetime and interaction cross section, and the singlet's cross section with pions. (The singlet state is the physical J/ψ state.) This parameterization is fixed with the p+A and A+B data from NA38 and NA50.

4.1 Calibration of the Three Parameters

Using the SPACY model of J/ψ production, which has the two state production included, there are three parameters required to describe the production and absorption of the J/ψ. It was discovered that these three parameters: σ_{octet}, τ_{octet},

and $\sigma_{J/\psi-\pi}$ had to be determined simultaneously. Recall from Chapter 2 that the J/ψ's existence is split into two stages: preresonance and physical J/ψ. The J/ψ's cross section for interaction is the sum of two step functions,

$$\sigma_{J/\psi} = \sigma_{octet}\theta(\tau_{octet} - t) + \sigma_{J/\psi}\theta(t - \tau_{octet}). \tag{4.1}$$

The preresonance state forms a rectangle with a height of σ_{octet} and width of τ_{octet}. The physical J/ψ forms a separate rectangle that has a height of $\sigma_{J/\psi}$ and width τ. We already classified the first three quantities as parameters, but τ is dependent on τ_{octet}. The relationship is given by

$$\tau = \tau_o - \tau_{octet}, \tag{4.2}$$

where τ_o is the amount of time from when the $c\bar{c}$ is formed until the J/ψ exits the collision region. We also know $\sigma_{J/\psi}$, the full cross section. The relationships between all the charmonium cross sections, are shown below. The relationships between the cross sections involving comovers use geometric arguments. To obtain charmonium cross sections with nucleons, one uses the additive quark model. It simply states that there is a factor of $\frac{3}{2}$ in obtaining the nucleon cross section, because there are three quarks in the baryons and only two in the mesons, *i.e.* pions.

$$\begin{aligned}
\sigma_{J/\psi-\pi} &= \sigma_c & &\simeq 1.0 \text{ mb}, & \sigma_{J/\psi-N} &= \tfrac{3}{2}\sigma_{J/\psi-\pi} &\simeq 1.50 \text{ mb} \\
\sigma_{\psi'-\pi} &= \sigma_c \left(\frac{r_{\psi'}}{r_{J/\psi}}\right)^2 &\simeq 3.68 \text{ mb}, & \sigma_{\psi'-N} &= \tfrac{3}{2}\sigma_{\psi'} &\simeq 5.52 \text{ mb} \\
\sigma_{\chi-\pi} &= \sigma_c \left(\frac{r_{\chi_c}}{r_{J/\psi}}\right)^2 &\simeq 2.4 \text{ mb}, & \sigma_{J/\psi-N} &= \tfrac{3}{2}\sigma_{\chi_c-\pi} &\simeq 3.6 \text{ mb}
\end{aligned}$$

Then,we produced data from SPACY with various values for the three parameters to determine the minimum χ^2 value for the fit of SPACY's predictions to the data. We produced collisions of p+p, p+^{10}B, ^{10}B+^{10}B, ^{32}S+^{32}S, and ^{100}Ru+^{100}Ru for SPACY's data, because they are approximately equally spaced in terms of AB. It was decided to use survival probability, S as the output from SPACY, because it can be calculated within SPACY. The equation used is

$$S = \frac{\text{Number of J}/\psi \text{ that survived}}{\text{Number of J}/\ \psi \text{ that would have been created}}. \tag{4.3}$$

SPACY is capable of calculating the probability that a $c\bar{c}$ pair will produce a J/ψ. Thus, any octet state or higher charmonium that is dissociated and would have become a J/ψ is accounted for in the calculation of S. The data was collected by NA38 and NA50 and includes p+A and A+B data, which was converted from cross sections to survival probabilities. This procedure is done by assuming that for p+p collisions $S = 1$. This gives us the equation

$$S = \left(\left.\frac{B_{\mu\mu}\sigma(J/\psi)}{\sigma(DY)}\right|_{AB}\right) / \left(\left.\frac{B_{\mu\mu}\sigma(J/\psi)}{\sigma(DY)}\right|_{pp}\right). \tag{4.4}$$

Table 4.1: Table of experimental data for p+A and A+B data obtained from [1].

Reaction	$\mathbf{p_{beam}(AGeV/c)}$	**AB**	$\mathbf{B_{\mu\mu}\sigma(J/\psi)/AB(nb)}$	**S**
p+p	450	1	2.22 ± 0.15	1.00 ± 0.10
p+d	450	2	2.31 ± 0.16	1.04 ± 0.10
p+C	450	12	1.89 ± 0.14	0.85 ± 0.09
p+Al	450	27	1.69 ± 0.14	0.76 ± 0.08
p+Cu	450	63	1.71 ± 0.13	0.77 ± 0.08
p+Cu	200	63	1.78 ± 0.41	0.88 ± 0.19
p+W	450	184	1.52 ± 0.11	0.69 ± 0.07
p+W	200	184	1.51 ± 0.15	0.68 ± 0.08
p+U	200	238	1.48 ± 0.35	0.67 ± 0.16
O+Cu	200	1008	1.35 ± 0.17	0.61 ± 0.09
O+U	200	3808	1.26 ± 0.16	0.57 ± 0.08
S+U	200	7616	1.08 ± 0.11	0.49 ± 0.06
Pb+Pb	158	43100	0.71 ± 0.05	0.32 ± 0.03

The data is shown in Table 4.1.

Once the method of data obtainment was set, the method of how to determine the best set of parameters, we have to determine how to find the minimum χ^2 value. We know the theoretical predictions for these values are: σ_{octet} = 6 - 7 mb, τ_{octet} = 0.25 - 0.3 fm/c, and $\sigma_{J/\psi-\pi}$ = 2.5 - 3 mb [46]. One would assume that the best course of action would be to create a three dimensional space, where each axis represents one of the parameters. Then, change only one parameter at a time to find a minimum on each axis. The final step would be combining these values with new ones (near the minimum values) to determine the set of parameters with the minimum χ^2. This method does not work in this situation, because the two octet parameters are coupled. The suppression of the octet is related to the

product of the lifetime and cross section. Recall, the picture described above of the plot of cross section versus time. We have two rectangles representing the preresonance and physical J/ψ state. If we assume that each rectangle has area A_1 and A_2, repectively. Then, we can assume $A_1 + A_2 \simeq$ const. Inserting values for these areas, we get

$$\sigma_{octet}\tau_{octet} + \sigma_{J/\psi}(\tau_o - \tau_{octet}) \simeq \text{const.}, \tag{4.5}$$

where τ_o is the time from $c\bar{c}$ creation to the J/ψ exiting the collision region. One can see that there are many solutions that can satisfy this equation. This method determined the values of the parameters used to try to fit the NA50 data.

It was decided that we would fit the experimental data to an equation for the AB dependence of the survival probability. To first order, we can rewrite the survival probability as

$$S = \frac{\sigma_{surv}}{\sigma_{prod}} = \frac{D(AB)^{\alpha}}{F(AB)} = C(AB)^{\alpha-1}, \tag{4.6}$$

where C, D, and F are constants, AB is the product of the atomic masses of the target and projectile, and α is a variable representing the suppression[1]. The value for C was fixed to be 1, since we assumed the $S = 1$ for p+p collisions. This

[1] $\alpha = 1$ means that there is no suppression, $\alpha < 1$ means there is suppression in production, and $\alpha > 1$ means there is an enhancement in production.

allowed us to find α for the experimental data. Each set of SPACY data was created with different sets of the three parameters. We then find an α value for each set of SPACY data produced. Then, we calculate the fit value of S for each data point from Eqn. 4.6. Finally, we calculate the χ^2 value from

$$\chi^2 = \sum_i \left(\frac{\text{data(S)} - \text{fit(S)}}{\sigma_S} \right)^2, \tag{4.7}$$

where σ_S is the error of S from the fit to the data, fit(S) is the S from the experimental data fit, and data(S) is the S from the SPACY data fit. The number of degrees of freedom is equal to the number of data points minus the number of fitting parameters. In this analysis, the DOF = 10 since there are 13 data points and three parameters.

The results of this process are shown in Fig. 4.1. The χ^2 /DOF = 4.86 for the parameter set (theoretical values): σ_{octet} = 6 mb, τ_{octet} = 0.3 fm/c, and $\sigma_{J/\psi-\pi}$ = 2 mb. We can see from the plot that the p+p, p+A, and light A+B data can be fit by these values, but the Pb+Pb point falls approximately 5 standard deviations below the fit line. The unique nature of this problem did not allow for a systematic search for the best values for the parameters. Instead, the parameters were found fixing two parameters close to theoretical predictions and adjusting the third. The two set variables were $\sigma_{J/\psi-\pi}$ and τ_{octet}.

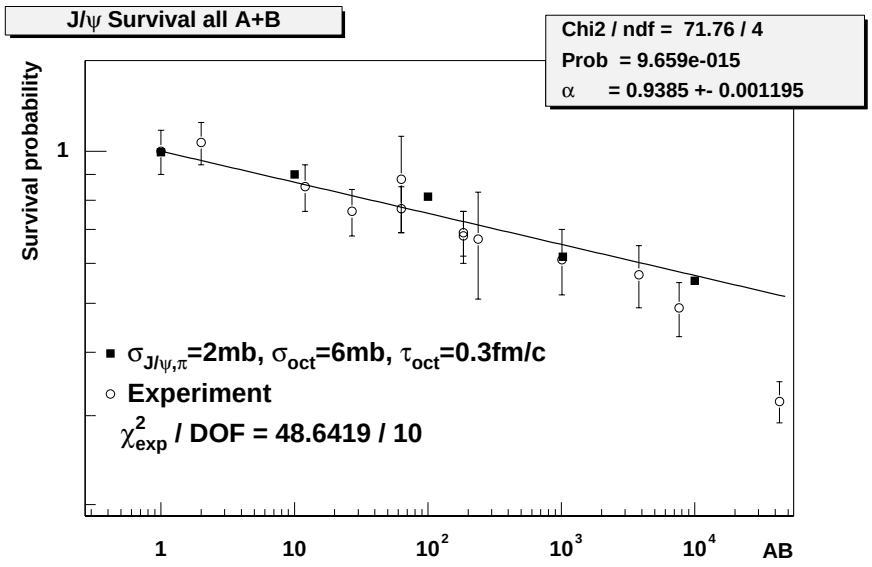

Figure 4.1: SPACY predictions and NA50 data for survival probabilities versus AB.

Table 4.2: Table of χ^2 values for fits with various parameter sets to parameterize the J/ψ production for 10,000 SPACY events.

$\sigma_{\mathbf{J/\psi-\pi}}\mathbf{(mb)}$	$\sigma_{\mathbf{octet}}\mathbf{(mb)}$	$\tau_{\mathbf{octet}}\mathbf{(fm/c)}$	$\chi^{\mathbf{2}}\mathbf{/DOF(withPb+Pb)}$
4.0	**1.6**	**0.3**	**1.22**
0.1	16	3	1.33
2.0	6.0	0.3	4.86

As discussed above, there is a problem of the interdependence of the three parameters. We would expect that long lifetimes and high cross sections for the octet coupled with a small comover cross section will fit the data equally well as a large comover contribution, a small octet lifetime, and a small octet cross section. This behavior is observed in SPACY as can be seen in Table 4.2. Two of the these other parameter sets are shown in Figures 4.2 and 4.3. This data shows us

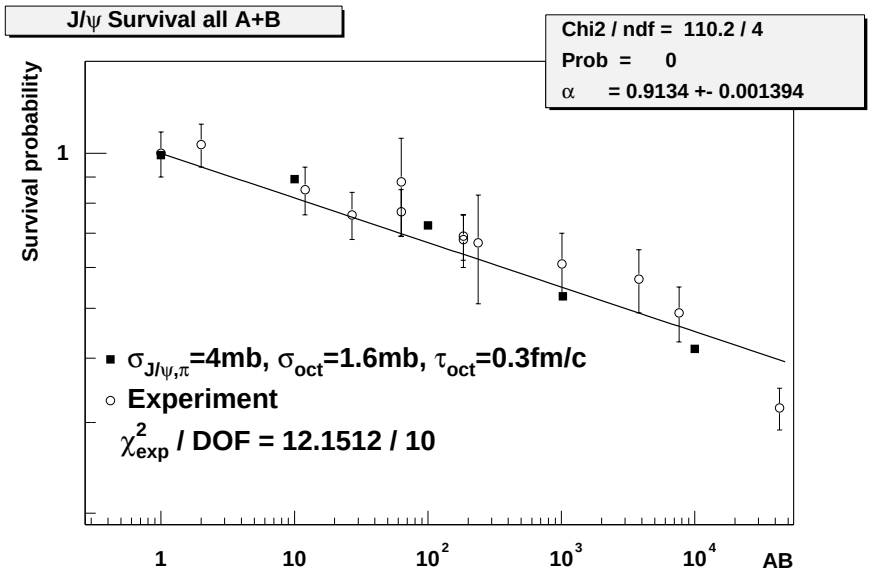

Figure 4.2: SPACY predictions and NA50 data for survival probabilities versus AB with a high octet contribution to the suppression.

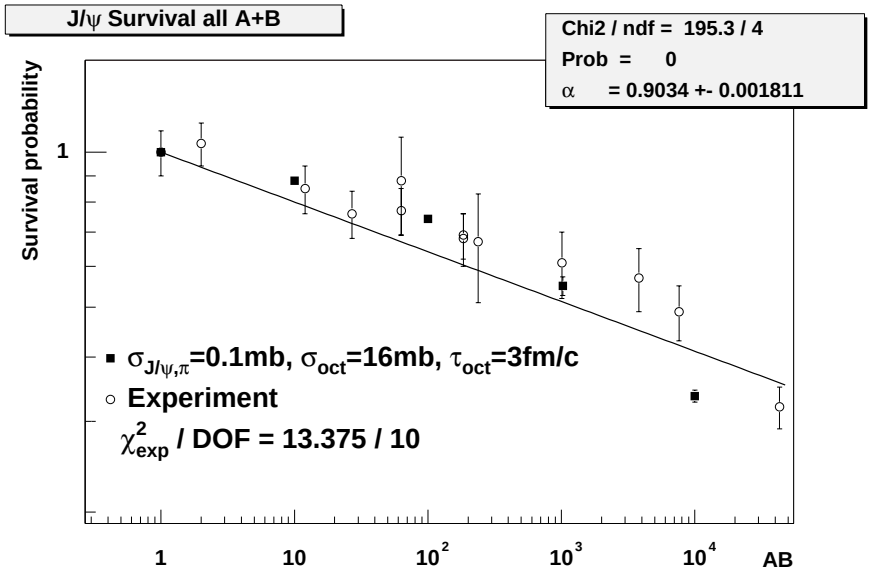

Figure 4.3: SPACY predictions and NA50 data for survival probabilities versus AB with a high singlet contribution to the suppression.

Table 4.3: Table relating contributions from the various sources of absorption for the J/ψ in Pb+Pb collisions at 158 A GeV/c.

DestructionMethod	**Contribution**
Projectile Nucleons	$35.2 \pm 1.6\%$
Target Nucleons	$37.1 \pm 1.6\%$
Produced Nucleons	$4.7 \pm 0.7\%$
Produced Mesons (Comovers)	$23.0 \pm 1.4\%$

that with the NA50 data alone we cannot determine the contribution of the octet and singlet states to J/ψ absorption. The second set of parameters was chosen to further study the E_T results, because its values are consistent with the theory [46] and are not overly biased to one source of suppression, octet or singlet. This set also shows moderation between the octet and singlet contribution, so one source of absorption is not biased in the rest of the analysis. The full space-time development of the nucleus-nucleus collision available in SPACY gives us an excellent oppportunity to study the contributions of various sources of absorption. For the chosen parameter set in Pb+Pb collisions at 158 A GeV/c, the contributions are shown in percentages for J/ψ destruction by projectile nucleons, target nucleons, produced nucleons, and comovers (Table 4.3). The numbers show that comover absorption is nontrivial in the SPACY model of J/ψ absorption. This means that the comovers cannot be ignored in the hadronic absorption scenario.

4.2 Analysis with Transverse Energy Distributions

NA50 observes a threshold in the ratio of the J/ψ cross section to the Drell-Yan cross section as a function of E_T. Their interpretation is that the threshold represents the phase transition from hadronic matter to the quark-gluon plasma [1]. There are two phases to this analysis. First, the ratio of the cross sections was obtained by finding the distributions of $\frac{d\sigma}{dE_T}$ for both the dimuons from the Drell-Yan process and the muons from the decay of a J/ψ. A simple division of these values yields the final ratio reported, $B_{\mu\mu}\sigma(J/\psi)/\sigma(DY)$. However, the problem was how the Drell-Yan distribution was obtained. There are statistical fluctuations in the Drell-Yan distribution. NA50 explored an alternate analysis of the Drell-Yan data. In the second analysis, NA50 "smoothed" the Drell-Yan distribution with tail of the minimum bias E_T distribution. With this method, they still observe a threshold. A second, and arguably better analysis technique, produced the same result. This lends more credence to their original conclusion about the presence of a threshold.

In Section 3.6, we discussed SPACY's reproduction of the minimum bias distribution as measured by NA50 (their electromagnetic calorimeter has an acceptance of $1.1 < \eta < 2.3$). We analyzed the E_T distribution of 10,000 Pb+Pb collisions where J/ψ mesons were produced. The SPACY results are plotted with the NA50 data [47] in Fig 4.4.

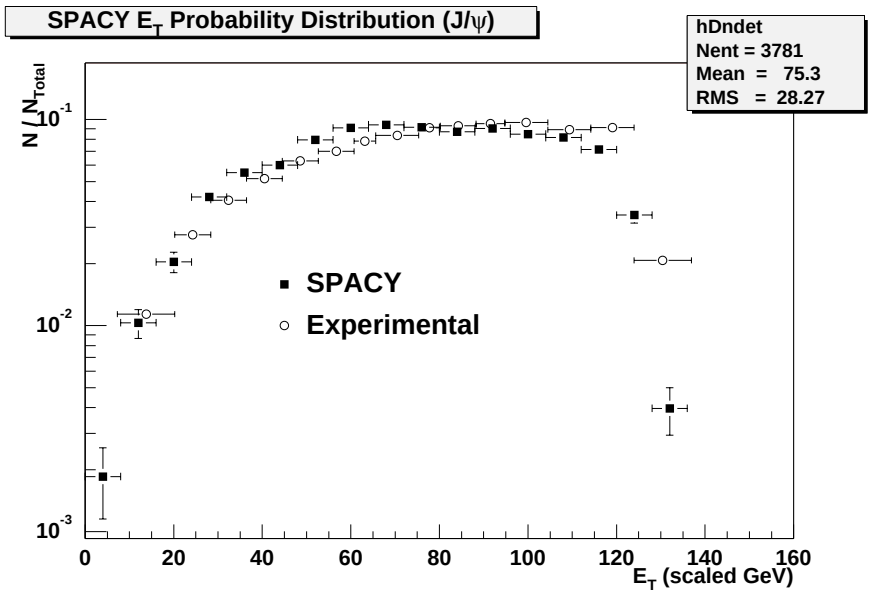

Figure 4.4: SPACY predictions and NA50 data for the E_T distribution of events where a J/ψ is present.

A comparison was done to the E_T distributions. Instead of calculating the ratio of the J/ψ cross section to the Drell-Yan cross section, we calculated the survival probabilities. The conversion was done using the same method as converting the values in Table 4.1. The data from the "Drell-Yan" smoothed analysis is shown in Table 4.4 and the data from the "minimum bias" smoothed analysis is shown in Table 4.5. Only the minimum bias data set is plotted with the SPACY data in Fig. 4.5

Table 4.4: Table of experimental data E_T and survival probabilities obtained from the Drell-Yan E_T data "smoothed" from the theoretical predictions [1].

$\langle \mathbf{E_T} \rangle (\mathbf{GeV})$	$\mathbf{B}_{\mu\mu}\sigma(\mathbf{J}/\psi)/\sigma(\mathbf{DY})$	$\mathbf{S}$
14	35.8 ± 2.6	0.73 ± 0.10
24	28.2 ± 2.2	0.58 ± 0.08
32	26.0 ± 1.7	0.53 ± 0.07
41	24.2 ± 1.4	0.50 ± 0.06
49	18.6 ± 1.0	0.38 ± 0.05
56	18.0 ± 1.0	0.37 ± 0.05
63	16.7 ± 1.0	0.34 ± 0.04
70	18.0 ± 1.0	0.37 ± 0.05
77	16.7 ± 1.0	0.34 ± 0.04
83	13.5 ± 1.1	0.28 ± 0.04
90	14.4 ± 0.9	0.30 ± 0.04
97	16.1 ± 1.1	0.33 ± 0.04
103	16.6 ± 1.3	0.34 ± 0.05
110	14.1 ± 1.1	0.29 ± 0.04
119	13.7 ± 1.3	0.28 ± 0.04

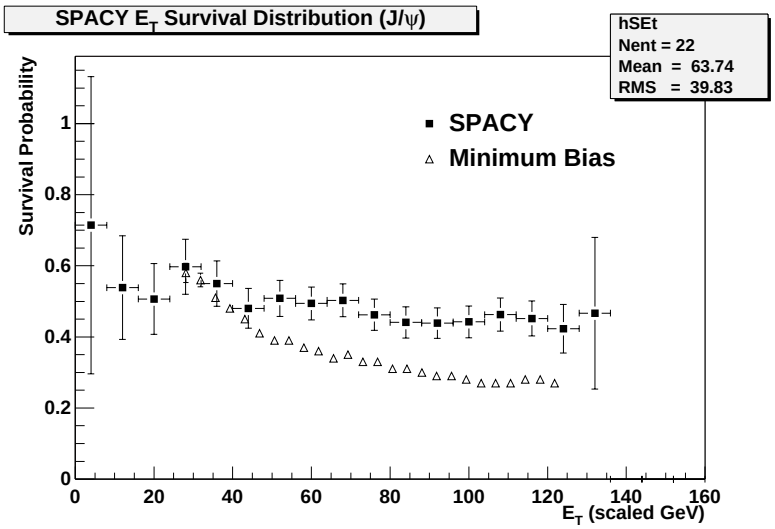

Figure 4.5: SPACY predictions and NA50 data for J/ψ survival probabilities versus E_T. This plot contains data "smoothed" with the minimum bias technique. The error bars for the most of the NA50 data are no larger than the symbols.

Table 4.5: Table of E_T values and survival probabilities calculated from [1] for the Drell-Yan E_T distribution "smoothed" by the minimum bias E_T distribution.

$\langle \mathbf{E_T} \rangle \mathbf{(GeV)}$	$\mathbf{B}_{\mu\mu}\sigma(\mathbf{J}/\psi)/\sigma(\mathbf{DY})$	$\mathbf{S}$
28.1	28.1 ± 1.3	0.58 ± 0.027
31.8	27.2 ± 0.9	0.56 ± 0.019
35.6	24.9 ± 0.6	0.51 ± 0.014
39.3	23.6 ± 0.5	0.48 ± 0.012
43.1	21.7 ± 0.4	0.45 ± 0.010
46.8	20.0 ± 0.3	0.41 ± 0.008
50.6	19.1 ± 0.3	0.39 ± 0.007
54.3	18.8 ± 0.3	0.39 ± 0.007
58.1	18.2 ± 0.3	0.37 ± 0.007
61.8	17.5 ± 0.3	0.36 ± 0.007
65.6	16.7 ± 0.3	0.34 ± 0.007
69.3	17.0 ± 0.3	0.35 ± 0.007
73.1	16.1 ± 0.3	0.33 ± 0.007
76.8	16.0 ± 0.3	0.33 ± 0.007
80.6	15.2 ± 0.3	0.31 ± 0.007
84.3	15.2 ± 0.3	0.31 ± 0.007
88.1	14.7 ± 0.3	0.30 ± 0.007
91.8	14.3 ± 0.3	0.29 ± 0.007
95.6	13.9 ± 0.2	0.29 ± 0.007
99.3	13.8 ± 0.3	0.28 ± 0.007
103.1	13.0 ± 0.3	0.27 ± 0.007
106.8	13.3 ± 0.3	0.27 ± 0.007
110.6	13.4 ± 0.3	0.27 ± 0.007
114.3	13.6 ± 0.4	0.28 ± 0.009
118.1	13.6 ± 0.5	0.28 ± 0.011
121.8	13.3 ± 0.7	0.27 ± 0.015

4.3 Comparison to "Anomalous" Suppression Results

As discussed in Chapter 2, the NA50 experiment has reported an "anomalous" suppression of J/ψ mesons in central Pb+Pb collisions at 158 A GeV. Here "anomalous" means beyond what is expected and in this context it is beyond what is expected in hadronic matter due to nuclear and comover absorption. As we saw in the in Figure 4.1, the Pb+Pb point falls well below the line that fits the SPACY data. Since the SPACY data fit line lies almost entirely on top of the experimental fit line, we can see that SPACY produces the proper level of suppression to explain this data. The range of agreement is from p+p collisions through S+U collisions. If we look at Figure 2.6, which is NA50 data [5], we see that the SPACY data fit line is nearly identical to the line that represents normal nuclear absorption as calculated by NA50.

To summarize, the theoritical values for cross sections and lifetimes in the SPACY model cannot fit the data of p+p through S+U and simultaneously fit the Pb+Pb point. Thus, SPACY cannot produce the level of suppression for Pb+Pb as is observed by NA50 [1, 5].

4.4 Comparison to E_T Threshold

As discussed in Chapter 2, NA50 reports a threshold in the E_T distribution of the ratio of the J/ψ cross section to the cross section for the Drell-Yan dileptons [1].

However, the Drell-Yan "smoothed" E_T distribution which shows the threshold in question is not completely reliable since the Drell-Yan distribution is subject to statistical fluctuations. There are not many of these high mass dilepton pairs in the data sample. Thus, SPACY does not rely on the Drell-Yan process to calculate the E_T distribution of the J/ψ mesons. We see in Fig. 4.4 that SPACY can come very close to reproducing the distribution for the J/ψ. However, as observed in Figure 4.5, SPACY cannot reproduce the magnitude of suppression as observed in Pb+Pb collisions by the NA50 collaboration. Also, we cannot explain the observed threshold with the SPACY model. Our comparison is weak in the low E_T region due to low statistics.

Chapter 5

Summary

In this thesis, we set out to use a computer code, SPACY, that represents a strictly hadronic model of high energy nucleus-nucleus collisions. It was used to study J/ψ production and absorption and attempted to explain the recent NA50 results [5, 1] with the hadronic model within SPACY.

5.1 Does the Hadronic Scenario Work?

As we saw in Chapter 4, the comovers are a necessary part of the hadronic scenario. They contribute on the order of 20% to the absorption in a SPACY simulation of Pb+Pb collisions. We also saw that with a low comover contribution, the octet contribution must be greatly increased to be able to still fit the p+p through S+U data from NA50.

From this work, we were able to learn about the preresonance state, especially

the cross section and lifetime. We determined that a shallow minimum in the χ^2 values, which allows an increase in one of the parameters to be compensated by a decrease in another. We see this when a high octet contribution to the absorption and low singlet (comover) contribution provide approximately an equal fit to a low octet contribution and a high singlet contribution. We also found that the parameters within the predicted range from Kharzeev and Satz, who advocate the preresonance state in their J/ψ production model [46], cannot fit all of the NA50 data ($\chi^2 = 4.86$).

With the hadronic scenario employed in SPACY, one does not expect to fit the Pb+Pb point. With the current model, we are not able to reproduce the magnitude of J/ψ suppression of the Pb+Pb collisions in the AB and E_T distributions. The octet and pion comovers should and do give a linear suppression in terms of AB, as shown in the Figures 4.1, 4.2, and 4.3. To obtain a nonlinear suppression, one that has a drop at high values of AB, we need more complexity in our hadronic scenario. Even though there is still more to be done, this thesis has laid the foundation for this continuing work.

5.2 Final Thoughts and Future Work

Even though the results from this thesis answered some questions, they also raised questions in the process. Open questions include an investigation of the x_F de-

pendence of the E866 p+A data, a study of the rescattering process, and a study of the ψ' suppression which starts in S+U collisions. This study could also be extended to study hadronic absorption at the Relativistic Heavy Ion Collider, RHIC.

Even though we could not explain the "anomalous" suppression with our hadronic scenario, it does not mean that we have confirmed a quark-gluon plasma formation. It is possible that a more sophisticated comover model could provide the nonlinear nature to the suppression that is observed in the NA50 data. Also, current work is being carried out by T. Barnes (Tennessee) and C.Y. Wong (ORNL) to make calculations for the J/ψ cross sections with the pion and rho mesons. There is also the possibility that inclusion of partonic effects could also produce this nonlinear nature. These topics could improve on the work performed for this thesis.

Further data is needed to resolve the ambuiguity of the octet versus singlet contributions to the absorption. I hope that more data from the PHENIX and STAR experiments at RHIC will improve the situation. RHIC is capable of producing p+p, p+A, and A+B collisions of different species at various energies. With the increasing energies, the density of comovers also increases. Thus, a good systematic study of J/ψ suppression as a function of the number of comovers can be conducted.

I have enjoyed my work on this thesis very much. Since 1995, I have believed

that J/ψ suppression is one of the most promising signals for observing quark-gluon plasma formation. Even though it is difficult to confirm a negative or "disappearance" signal, this is one of the few signals that reveals the initial state of a nucleus-nucleus collision. I hope this work contributes in some way to the effort on both the experimental and theoretical fronts.

Bibliography

Bibliography

[1] M.C. Abreu et al. *Phys. Lett.*, B450:456–466, 1999.

[2] F. Abe et al. *Phys. Rev. Lett.*, 79:572–577, 1997.

[3] D.M. Alde et al. *Phys. Rev. Lett.*, 66:133–136, 1991.

[4] M. Leitch for the E866 Collaboration. Talk presented at Quark Matter '99, to be published in Nucl. Phys. A.

[5] M.C. Abreu et al. *Phys. Lett.*, B410:337–343, 1997.

[6] N. de Marco for the NA50 Collaboration. To appear in the Proceedings of "Hadron Structure 98", Stara Lesna, Slovak Republic, September 7-13, 1998.

[7] Particle Data Group. *Eup. Phys. J.*, C3:1, 1998.

[8] C.Y. Wong. *Introduction to High-Energy Heavy-Ion Collisions.* World Scientific, Singapore, 1994.

[9] J. Rafelski. *Phys. Rep.*, 88:331, 1982.

[10] P. Koch, B. Müller, and J. Rafelski. *Phys. Rep.*, 142:167, 1986.

[11] G.E. Brown, C.M. Ko, Z.G. Wu, and L.H. Xia. *Phys. Rev.*, C43:1881, 1991.

[12] R. Mattielo et al. *Nucl. Phys.*, B24:221, 1991.

[13] J. Kapusta, P. Lichard, and D. Siebert. *Phys. Rev.*, D44:2774, 1991.

[14] R. Santo for the WA80 Collaboration. *Nucl. Phys.*, A566:61c, 1994.

[15] D. Irmscher for the NA45/CERES Collaboration. *Nucl. Phys.*, A566:347c, 1994.

[16] T. Matsui and H. Satz. *Phys. Lett.*, B178:416, 1986.

[17] C. Baglin et al. *Phys. Lett.*, B220:471–478, 1989.

[18] S. Gavin and R. Vogt. *Phys. Rev. Lett.*, 78:1006–1009, 1996.

[19] S.A. Bass et al. nucl-th/9711032.

[20] J.J. Aubert et al. *Phys. Rev. Lett.*, 33:1404, 1974.

[21] J.E. Augustin et al. *Phys. Rev. Lett.*, 33:1406, 1974.

[22] C. Baglin et al. *Phys. Lett.*, B255:459–465, 1991.

[23] C. Gerschel and J. Hüfner. *Phys. Lett.*, B207:253–256, 1988.

[24] C. Gerschel and J. Hüfner. *Nucl. Phys.*, A544:513c–516c, 1992.

[25] C. Gerschel and J. Hüfner. *Z. Phys.*, C56:171–174, 1992.

[26] R.L. Anderson et al. *Phys. Rev. Lett.*, 38:263, 1977.

[27] S. Gavin, M. Gyulassy, and A. Jackson. *Phys. Lett.*, B207:257–262, 1988.

[28] R. Vogt, M. Prakash, P. Koch, and T.H. Hansson. *Phys. Lett.*, B207:263–268, 1988.

[29] R. Vogt. *Phys. Lett.*, B430:15–22, 1998.

[30] E. Braaten and S. Fleming. *Phys. Rev. Lett.*, 74:3327–3330, 1995.

[31] D. Kharzeev, C. Lourenço, M. Nardi, and H. Satz. *Z. Phys.*, C74:307–318, 1997.

[32] F. Abe et al. *Phys. Rev. Lett.*, 79:578–583, 1997.

[33] Proceedings of the "Charmonium Production in Relativistic Nuclear Collisions" workshop. Published by the Institute of Nuclear Theory, University of Washington, Seattle.

[34] Proceedings of the quark matter '97 conference. Published in Nucl. Phys. A638.

[35] Proceedings of the quark matter '99 conference. To be published in Nucl. Phys. A.

[36] D. Kharzeev and H. Satz. Colour deconfinement and quarkonium dissociation. In R.C. Hwa, editor, *Quark-Gluon Plasma 2*, pages 395–453. World Scientific, 1995.

[37] J. Hüfner and B. Kopeliovich. *Phys. Lett.*, B445:223–231, 1998.

[38] J. Geiss, E. Bratkovskaya, W. Cassing, and C. Greiner. nucl-th/9810059.

[39] S.P. Sorensen. SPACY version 6.1, 1999.

[40] S.P. Sorensen and W.-Q. Chao. *Commun. Theor. Phys.*, 21:317–326, 1994.

[41] R. Vogt. *Atomic Data, Nuclear Data Tables*, 50:343, 1992.

[42] N. Craigie. *Phys. Rep.*, 47:1, 1978.

[43] T. Alber et al. *Phys. Rev.*, C44:2736–2752, 1991.

[44] S.P. Sorensen. private communications.

[45] F. Bellieche. Thesis, Université Claude Bernard Lyon, 1997.

[46] D. Kharzeev and H. Satz. *Phys. Lett.*, B366:316–322, 1996.

[47] L. Ramello for the NA50 Collaboration. *Nucl. Phys.*, A638:261c–278c, 1998.

Vita

Samuel Held was born on April 13, 1974 in West Palm Beach, Florida. He graduated in 1992 from North Tonawanda High School in North Tonawanda, NY (north of Buffalo) with a Regents diploma with honors in Science, Mathematics, and Spanish. He then attended the University of Rochester for his undergraduate education. He started his work in the field of high energy nuclear physics with Dr. Frank Wolfs by working with him on the PHOBOS experiment's Time of Flight wall. He graduated from the University of Rochester in May of 1996 with a B.S. in Physics. On June eighth of 1996, he married Erica Ciaccia. They moved to Knoxville, TN for Samuel to begin graduate school in the Fall of 1996 at the University of Tennessee. He also began work with Dr. Soren Sorensen and Dr. Ken Read on the Muon Identifier for the PHENIX experiment at RHIC. On April 24, 1998 his son, Samuel Thomas, was born. In August of 1998, Samuel chose to pursue his teaching certification in Physics and Mathematics while completing a Masters degree in Physics. He received his Masters in Physics in August of 1999 and began his work towards his Masters in Education.